EUROPEAN ORGANIZATION FOR NUCLEAR RESEARCH

CERN --- AB DEPARTMENT

EURISOL-DS Multi-MW Target
A proposal for improving overall performance in relation to the isotope yield

**Karel Samec, Mats Lindroos, Yacine Kadi,
Roberto Rocca, Cyril Kharoua**

AB Dept. ATB

European Organization for Nuclear Research (CERN)

CH-1211 Geneva 23, Switzerland

Abstract

The Eurisol Design Study has been initiated by the European Commission to demonstrate the feasibility of a facility for producing large yields of exotic isotopes.

At the core of the projected facility, the neutron source produces spallation neutrons from a proton beam impacting dense liquid metal. The neutrons emitted from the source are used to fission Uranium targets which, in turn, produce high yields of isotopes.

This technical report summarises efforts to improve the overall performance of the planned facility, by optimising the neutron source and the disposition of the fission targets

Geneva, Switzerland

11 September, 2008

T a b l e   o f   C o n t e n t s

-

L i s t   o f   F i g u r e s

-

L i s t   o f   T a b l e s

-

L i s t   o f   S y m b o l s

-

Parameters, variables and abbreviations:

CEA	Abbr.	Commissariat à l'Energie Atomique, France
CERN	Abbr.	Centre Européen de la Recherche Nucléaire, Switzerland
C_P	[J/kg/K]	Thermal capacity
CFD	Abbr.	Computational Fluid Dynamics
dpa	Abbr.	Displacement per atom
FEM	Abbr.	Finite Element Method
FZK	Abbr.	Forschungszentrum Karlsruhe, Germany
f	[Hz]	Frequency
INFN	Abbr.	Instituto Nazionale de Fisica Nucleare, Italy
IPUL	Abbr.	Institute of Physics of the University of Latvia, Latvia
LM	Abbr.	Liquid Metal
PSI	Abbr.	Paul Scherrer Institute, Switzerland
RCCMR	Abbr.	CEA design rules for mechanical components of FBR nuclear islands
T	[°C]	Temperature
t	[sec.]	Time
Δ	[-]	Discrete difference, change
ϕ	[n/cm^3/s]	Neutron flux
λ	[W/m/s]	Thermal conductivity
ρ	[kg/m^3]	Density

R e f e r e n c e s

-

[Ref1]	Y. Blumenfeld: EURISOL : review of accelerators for radioactive beams		
	www.epac08.org/ MOZAM01	Proceedings of EPAC08, Genoa, Italy	June 2007

[Ref2]	R. Schneider: Production and identification of 100Sn		
	Z. Phys.- A 348, 241-242	Zeitschrift für Physik A	April 1994

[Ref3]	K. Samec: Design of the Eurisol converter target		
	TM-34-07-05	PSI Internal Project Note	July.2007

[Ref4]	J. Freibergs et al.: Engineering design and construction of a functional Hg – loop		
		IPUL annual report	April 2008

[Ref5]	C. Fazio et al.: The Megapie Test project, supporting research and lessons learned in a first-of-a-kind spallation target technology		
	NED-238, 1471-1495	Nuclear Engineering and Design	June 2008

[Ref6]	C. Rubbia: A realistic plutonium elimination scheme with fast energy amplifiers and thorium-plutonium fuel		
	CERN/AT/95-053 (ET)	CERN internal Note	December 1995

[Ref7]	O. Alyakrinskiy: EURISOL Fission Target Design adapting MAFF concept		
	04-25-2007-0010	INFN Project note	November 2007

[Ref8]	A. Herrera-Martinez: EURISOL-DS Multi-MW Target Comparative Neutronic Performance of the Baseline Configuration vs. the Hg-Jet Option		
	CERN/AB/ 2006-037 (ATB)	CERN internal note	February 2007

[Ref9]	A. Herrera-Martinez: EURISOL Multi-MW Target Preliminary Study of the Liquid Metal Proton-to-Neutron Converter		
		CERN internal note	April 2006

[Ref10]	E. Brun: Detail thermal stress analysis of EURISOL Fission targets - First concept		
	TM-34-07-02	PSI Internal note	May 2007

[Ref11]	K. Samec et al.: Test predictions for the converter target		
	CERN-AB-Note-2008-057 ATB	CERN Internal note	September 2008

1 Introduction

The study of isotopes is of particular importance to nuclear physics both from a theoretical point of view but also as an experimental tool in many related fields of physics. The Eurisol project was proposed [Ref1] as an isotope production facility intended to produce rare isotopes at sufficiently high rates to allow their use and characterisation. The project is supported by the European Commission along with 40 research institutes.

Current advances in computing power have enabled the development of codes to predict the behaviour of matter at the most elemental level. Yet such developments in the code lead to ever greater complexity and thus also require validated experimental data in ever increasing detail. Rare isotopes known as doubly magic as for instance Tin-100, are of particular interest [Ref2] as they combine stability of both the proton and neutron structure. Physicists hope that calibrating their codes with such isotopes can give them new insight into predicting the behaviour of isotopes far off from the valley of stability. The possible appearance of rare isotopes with an abundance of protons versus neutrons such as Nickel 48 with 28 protons and just 20 neutrons could also give new insight into the interactions between nucleons and improve the physicist's understanding of matter. It is not known today whether such an isotope could form or whether it is too far from the speculated proton drip-line. In the same manner there is speculation over the existence of a neutron drip-line beyond which neutrons can no longer form such as past Lithium 11.

Other scientific fields benefiting from the production of isotopes in large amounts include both the applied sciences in materials research such as magnetism or super-conductivity, but also astro-physics for the study of nucleo-synthesis in stars. Nuclear medicine has made great progress and the scope for improving the effectiveness of treating cancer patients would equally benefit from access to larger yields of isotopes, including some who's scarcity have limited their use in clinical trials.

The only known method which may yield isotopes in greater number and variety is to increase the number of fissions in a target made of fissile material. Thus, by increasing the isotope yield, one hopes there would be a greater chance of observing the exotic isotopes in sufficient number and over a long enough period to characterise them in mass, energy and lifetime. The Eurisol project aims to achieve this goal with the design shown in Figure 1. Essentially, in this facility, a 1 GeV / 4 mA / 4 MW proton beam impacts a centrally located mercury-filled neutron spallation target which ejects highly energetic neutrons. Uranium Carbide fission targets are placed in the path of the neutrons exiting the mercury target thus producing isotopes by fission.
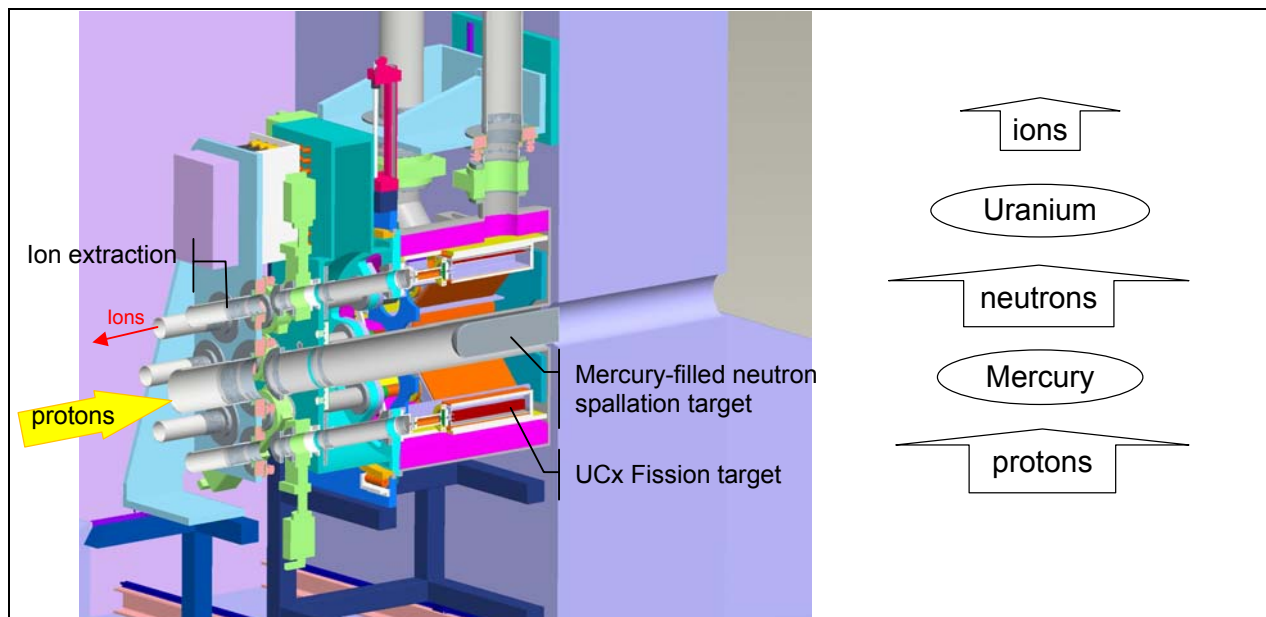
Figure 1: EURISOL general layout (left, INFN) and principle (right)

A proposal for improving overall performance in relation to the isotope yield

The fission targets have been studied by INFN-Legnaro and NIPNE which have considered a number of solutions for increasing fission yield, such as the use of highly enriched uranium or natural uranium, different concepts for the reflectors and various orientations of the fission targets. One possible configuration is shown surrounding the mercury neutron spallation target in Figure 1. The design of both the fission targets and neutron spallation target are closely related such that a global neutronic calculation of both targets is needed for an accurate prediction of the radioactive isotope yield.

The neutron spallation target is filled with liquid mercury which must be continuously circulated to evacuate the heat deposited by the proton beam which dumps approximately 60% of its power or 2.4 MW into the target. A hydraulic and mechanical design study by PSI and a neutronic evaluation by CERN have resulted in the baseline configuration [Ref3] shown in Figure 2 (left) which comes slightly below the stated objective of the entire projected facility currently defined as 10^{16} fissions per second.

An alternative design [Ref4] was therefore proposed in which a thin descending film of mercury would be impacted by the proton beam transversely as shown in Figure 2 (right). This concept would effectively double the number of fissions as the spallation neutrons have a shorter path to exit the mercury.

The Coaxial Guided Stream (CGS) design benefits from having been shown to work without interruption by the Megapie project which operated quite successfully over a period 4 months [Ref5] at beam powers up to 1 MW. However as a neutron source the CGS concept currently envisaged is less efficient at producing a hard neutron flux than the film design.

Both designs for the neutron source have been built and are being validated by the laboratory for liquid metals of the University of Latvia (IPUL) through a series of tests which will be completed by mid 2009.
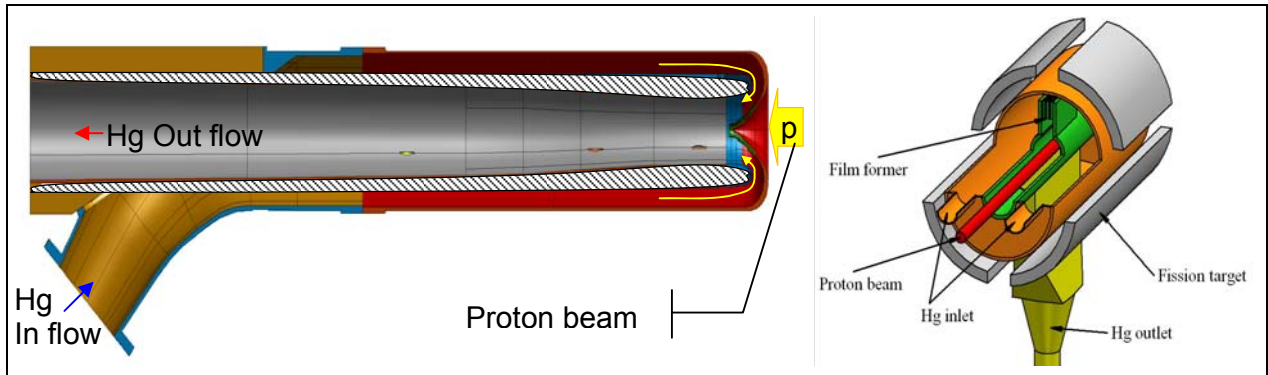
Figure 2: Design variants for the neutron source; CGS design (left, PSI) and film design (right, IPUL)

In a wider context, the demonstration of a 4 MW neutron spallation source will benefit the development of the subcritical reactor diversely known as energy amplifier or accelerator driven system (ADS) proposed by C. Rubbia of CERN [Ref6] . In this reactor concept a neutron source produces fission in a sub-critical core made of Thorium, thus multiplying a hundredfold the energy injected into the accelerator, but without the need to keep a chain reaction in check. Indeed, whereas in a conventional nuclear reactor, criticality is governed by the fraction of delayed neutrons, in an ADS the source term for the neutrons is a given parameter which can be chosen by the operator (Figure 3).

Figure 3: Effect on the power output of a reactor from a rapid reactivity change of 2.5 $ (1$ ~ 200pcm), corresponding to the sudden extraction of control rods [Ref.6].
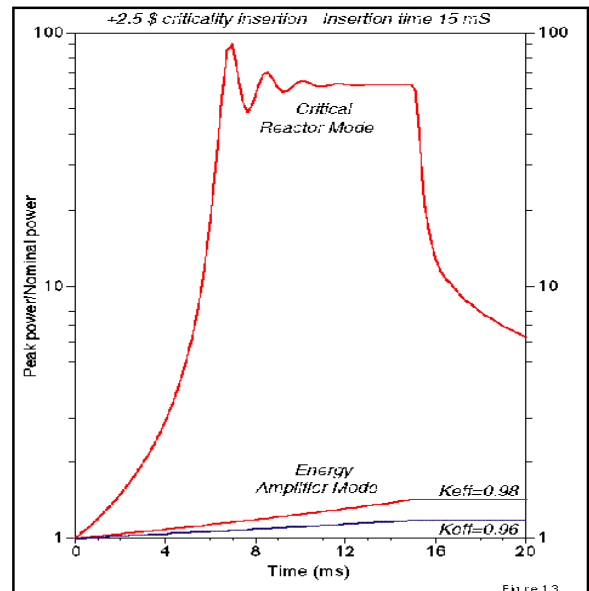
2 Scope

The current work will focus essentially on improving the neutronic performance of the closed target design as shown in Figure 2 (left). The main innovation proposed in this study is to integrate into the existing CGS design, one of the most attractive aspects of the film design, namely the short path in mercury for the neutrons. This may be achieved by integrating slits into the sides of the hull of the CGS design, and evacuating these slits to give neutrons exiting from the central neutron production area a more direct path to the fission targets with less matter to cross.

The proposed design change is illustrated in Figure 4 below, the lateral openings in the hull serve as a faster escape route for the neutrons produced in the centre of the source, whilst at the same time guiding the liquid metal in the outer annulus. It is thus hoped that the neutronic performance will be improved whilst at the same time minimising the pressure losses in the hydraulic circuit. The feasibility of manufacturing the proposed target has been verified internally at CERN and no difficulties with this concept have been uncovered.

The FLUKA code will be used to examine how best to maximise the neutron flux, in an energy spectrum susceptible to fission uranium, preferably natural or 4% enriched uranium. The code is a standard tool at CERN for neutronics; its main advantage is its ability to deal with high energy charged particles. The great variety of nuclear models contained in the code, lend it a degree of versatility in terms of the reactions it can simulate ensure that all possible aspects are covered form the protons entering the system to the neutrons leaving the source. The neutronic calculations will therefore be based on the CAD models of the proposed modified design. As customary with these types of codes, the geometry will be simplified.
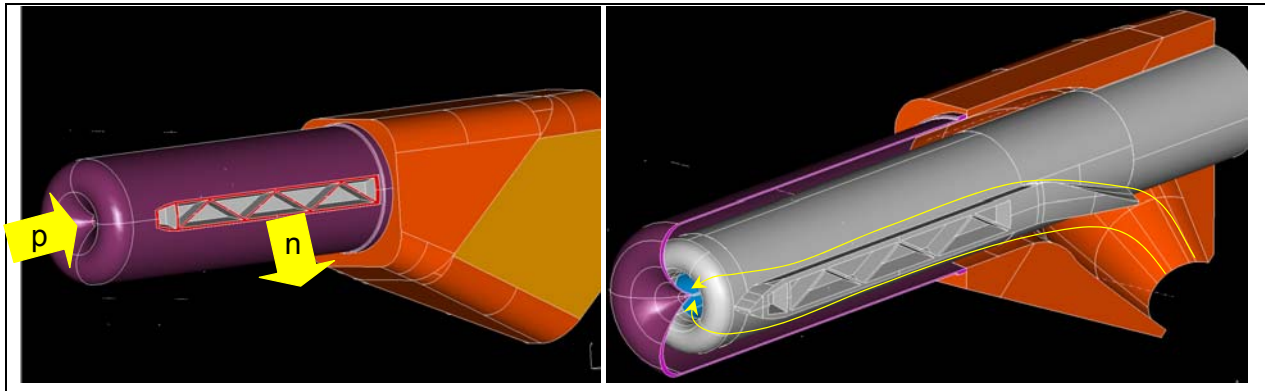
Figure 4: Proposed conceptual changes to the baseline design of the neutron source

As mentioned in the introduction, the neutronic calculation shall encompass the fission target and the surrounding structure, although the design of the fission targets *per se* is not the focus of the current work. The method retained in the study is to first optimise the design of the spallation target in terms of the neutron flux and spectrum, and then to integrate the fission targets into the calculation.

The challenge of this latter phase in the optimisation is to dispose the fission targets in the most favourable manner to enhance fission, taking into account cooling aspects as well as the need for extracting the ions, and not withstanding design constraints inherent to an engineering task. The fission targets modelled in this study will therefore reflect some of the proposed alternatives deemed most likely to enhance fission, notably some modifications in line with the design of the MAF fission target as proposed in [Ref7]. Various combinations of reflector blocks around the targets may also be envisaged.

The detail fluid-dynamic results in [Ref11] illustrate how best to modify the existing design hydraulically whilst improving the production of neutrons, in line with the idea shown in Figure 4. The motivation for the current analysis is therefore to learn from the analysis of the initial design to benefit both the production of neutrons whilst enhancing fluid dynamic stability.

3 Methods and tools

3.1 Iteration process

The process for improving the performance of the Eurisol isotope production facility has to follow a multi-facetted approach, as the neutronic aspects are directly linked to the hydraulic performance of the circulating metal. Moreover the very high liquid metal speed inside the neutron source has severe implications for the structure; in particular dynamic solicitations are bound to arise. An iterative process will therefore focus on alternating successive neutronic and fluid-dynamic analyses, interspersed with structural considerations.
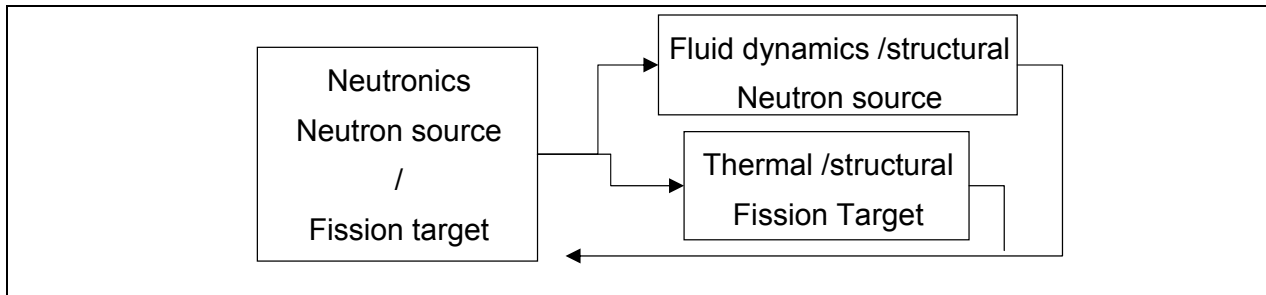
Figure 5: Iterative process for optimising the neutron source

The point of departure is the existing systems analysis as described in [Ref8] and [Ref9], completed by the fission target thermal/structural and fluid dynamic analyses in [Ref10], [Ref11] and the design report for the neutron source [Ref3]. For greater clarity, the current status is briefly summed up in the next few tables. The CGS design of the neutron source shown in Figure 2 must follow the baseline system characteristics listed in Table 1 and in accordance with the scheme in Figure 1. The compared neutronic performance of existing facilities is listed hereafter, the goal of the current project being to increase the fission yield markedly.

Parameter	Value
Primary particle beam	1 GeV / 4 mA / 4 MW proton
Neutron source dimensions	Diameter 15 cm / Length 40 - 100cm
Neutron yield	29 / primary
Neutron flux at source exit	$\sim 10^{14}$ n/cm^2/s/MW beam power
Spectrum hardness:	peak @ 1 MeV = 50 x peak @ 100 MeV
Isotopic yield:	$\sim 10^7$ - 10^8 isotopes /cm^3 /s /MW of beam
Fission density:	$\sim 10^{11}$ f /cm^3 /s /MW beam power

Table 1: Key parameters of the EURISOL baseline configuration

Facility	Institute	Beam particles	Beam Power	Number of fissions
SPIRAL-II	GANIL	Deuterons 40 MeV	200 kW	>5 10^{13}
HIE-ISOLDE	CERN	Protons 1.4 GeV	10 kW	10^{13}
SPES	Legnaro	Protons 40 MeV	8kW	10^{13}
EURISOL	-	Protons 1GeV	5 MW	>10^{15}

Table 2: Performance of comparable facilities

3.2 The FLUKA code

The FLUKA code solves the Boltzmann equation in phase space, for most applications limited to 7 fundamental variables comprising position momentum and time. Other dimensions reflecting quantum

numbers such as spin, may be envisaged but are not current. The process by which the solution is approximated relies on a Monte Carlo method of generating multiple particles at random in phase space and tracking their interactions until they are re absorbed or leave the system. The runs are grouped by batches of at least a few tens of thousands of individual particles; usually a minimum of 5 batches is required. The statistics on relevant detectors such as the fluence for instance, then give an indication as to whether enough particles have been tracked to ensure representative results have been produced. A figure of less than 10% for the variance is required.

The interactions programmed in the code are necessarily limited to the experimental data available. As such one of the stated goals which is to investigate the possible emergence of rare isotopes is not directly predictable, one can only hope to gauge the possible enlargement of the variety of isotopes which may be purportedly produced, but with no certainty.

At the deepest level, the code contains a model of the interaction between a hadron and a nucleus which provides reliable results up to energies in the order of tens of TeVs. These refinements include the latest developments in the field of string theory necessary for high energies above hundreds of MeVs and take into account the interaction of quarks. The duration of the interaction is very small, in the order of 10^{-22} seconds, after which all anti-nucleons have disappeared as well as all nucleons below 30 MeVs, either through scattering or absorption. There remains a nucleus in an excited state, which can then undergo evaporation (spallation), fragmentation or fission after some 10^{-20} seconds. The relative weight of each of the three exit modes is again modelled using experimental data. In particular as fission always competes against evaporation, the computational results are only as good as the data available over the vast energy ranges covered by the code and the equally great number of possible ejectiles. Another mechanism which may be considered with the code occurs at high energies above hundreds of MeVs; light fragments may be emitted through the coalescence mechanism: these are nucleons emitted in phase space near enough to be "put together". Finally 10^{-16} seconds after the initial interaction, γ de-excitation completes the process.

There remains a residual nucleus with a given composition and energy which may be used for activation studies or, as in our case, isotope production studies. At this step in the calculation any hadrons such as neutrons produced in the interaction are transported until they are captured and appear in the tally of fluence or escape from the system. The next particle generated by a Monte Carlo random number generator then goes through the same process but it does not interact with nuclei calculated by the code, Each particle track computed in Fluka is thus independent and studies of the evolution of reactivity induced by burn-up of nuclear fuel for instance are not directly possible.

The transport of neutrons is dependent on the cross-section data implemented. Fluka relies currently on a 260 group model below 20 MeV, which entails certain homogenisation for resonance regions. Point to point sectional data is available for a limited number of elements and may be selected although it is not activated by default to conserve CPU. This limitation is not viewed as an obstacle in the current project, as high energy fission is strived for, which should increase yield in the medium range atomic numbers around A=50. The influence of temperature on the cross-sectional capture properties is well known as "self-protection". These may be activated in Fluka, yet they remain relevant to the energies below several keVs.

Finally electro-magnetic effects, in particular pertaining to electrons are included in Fluka, although CPU intensive they cover not only pair production, photo-electric, Bremsstrahlung but also Coulomb scattering through a model known as Molière theory to approximate multiple scattering in a single step.

3.3   Choice of physics models

The type of fission which is most relevant to the current project is broadly dominated by high energies, in the order of MeVs. Point-to-point cross-sectional data will not be considered; the 260 groups for neutrons below 20 MeVs should suffice at the energy range being considered. Likewise, the hard spectrum of the neutrons as well as the absence of any "pure" materials entails that "self-shielding" need not be considered,.

The nature of the beam impacting the target, namely protons, dictates that electromagnetic effects be considered. This is particularly important for ionization losses in the target mercury and the appearance of the so-called Bragg peak, when protons reach a threshold value below which they cannot progress further into the target and deposit all their remaining energy at a point dependent on the initial momentum.

Models which will be considered for the current study include:

- Fission / fragmentation

- Evaporation

- Coalescence

- Electro-magnetic effects above 0.1 MeV

- Neutron transport in 72 groups below 19.6 MeV will be used in the initial optimisation.

> All the models presented in the study are computed with 5 batches of 50'000 particles which guarantee a variance well below 10% in all relevant energy bands.

3.4 Choice of materials

The Fluka library contains a selection of pure materials used in the current analysis, the materials are characterised from a nuclear standpoint by comparison with numerous test case and experimental data. Specific compounds such as uranium carbide are formed by the analyst on a case by case basis, by combining individual pure isotopes in the appropriate mass fraction or isotopic percentage.

Early on in the project, various analyses [Ref8] pointed to the fact that mercury as a target material would produce a harder spectrum, especially if were integrated within a thin target such as the film design. It was therefore preferred over Lead-Bismuth or Lead and has been retained in the current study. One of the consequences of this choice is that fast neutrons escaping from the central spallation region of the CGS target do undergo a little more thermalisation than with lead. It is therefore worth examining design changes which would mitigate this effect, whilst improving the overall hydraulic performance.

The choice of uranium carbide, over uranium oxide, for the fission targets is dictated by temperature constraints. The very high temperature reached in the fission target are needed to extract as much of the isotopes as possible. This is likely to happen well above 2000 °C which precludes the use of Uranium oxides. Furthermore, the porosity, grain size of UCx guarantees a faster diffusion/effusion process.

Another material of relevance is the reflector. In this instance Beryllium oxide is preferred, over a more traditional material such as carbon used in reactors. The reason is the hard spectrum of the neutrons and the need to limit thermalisation. Indeed, the reduced thickness of the BeO reflector makes it more effective than iron or carbon which have a higher Z number.

Name	Use	Isotopic composition (at%)	Specific gravity
Mercury	Spallation & cooling	100 % Hg	13.546
Beryllium Oxide	Reflector	50% Be 50% O	3.01
Uranium Carbide	Fission Target	0.37 % U235, 9.13 % U238 (=enriched 4%), 90.5% C	3.083
Natural Uranium Carbide	Fission Target	0.06 % U235, 9.15 % U238(=natural 0.7%), 90.78% C	3.083
Water	Cooling & reflector	0.66 % H 0.33 % 0	1.0
316 Stainless steel	Structure	62.24% Fe, 17.53% Cr, 15.95% Ni, traces	7.98
Tantalum	Heat shield	100% Ta	16.654
Carbon	Heat shield	100% C	2.0

Table 3: Materials List

4 Analysis of the neutron spallation source base design

4.1 Presentation of the base design

The base design as described in [Ref3] is presented below for completeness. Essentially, the liquid metal enters the target from below entering an off-axis diffuser inlet which distributes the fluid into the incomer, an annular-shaped tube between the guide tube and outer hull. At the beam window (right hand cone in the figure below), the liquid metal reverses direction through 180° at a point where it is impacted by the proton beam, it then exist the target down the outflow tube, from which it passes into a separate heat exchanger.

Side View:

Outer Hull

LM loop Interface & attachment

Annular Incomer

Hull Cut-away:

Guide Tube

Section view:

Flow reverser

Out flow

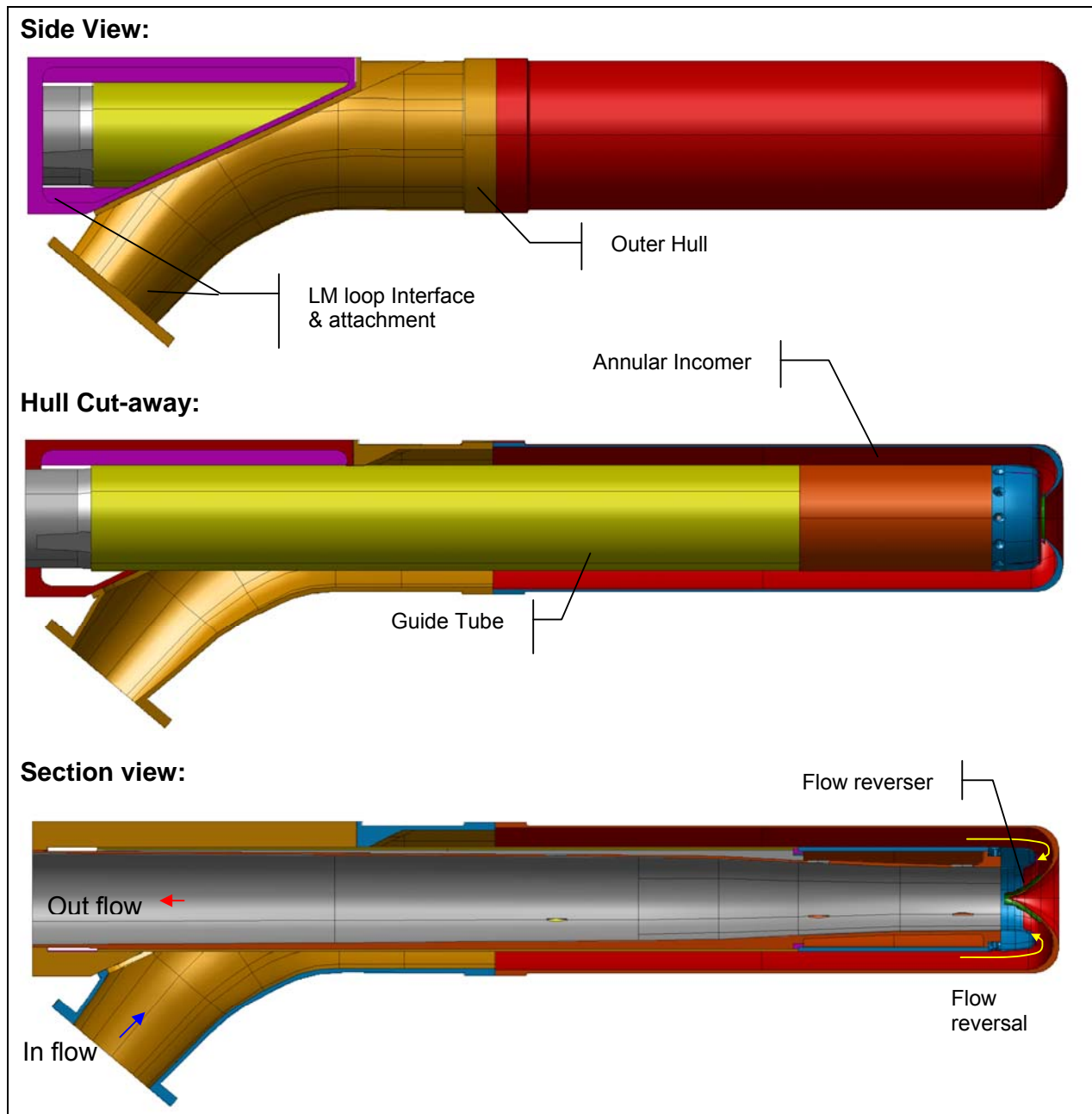**Flow reversal**

In flow

Figure 6: Base design of the neutron spallation target acc. [Ref3]

4.2 Fluka Model of the base design

4.2.1 Presentation of the model and verifications

The original model used in the early overall concept-level neutronic analysis of the target [Ref8] did not contain the hollow guide tube, a result of later design developments documented in [Ref3] shown in Figure 2 (left), and which may have an impact on the neutron yield and spectrum. Therefore it is important as a first step in the current study to implement relevant aspects of the latest design evolution of the target, in a more detailed neutronic model of the spallation target and most notably:

-   A detail model of the beam window, with a near-accurate thickness distribution.

-   Representation of the hollow guide tube used for purposes of thermal insulation

-   Accurate inlet and outlet placement and connection to mercury loop for shielding studies.
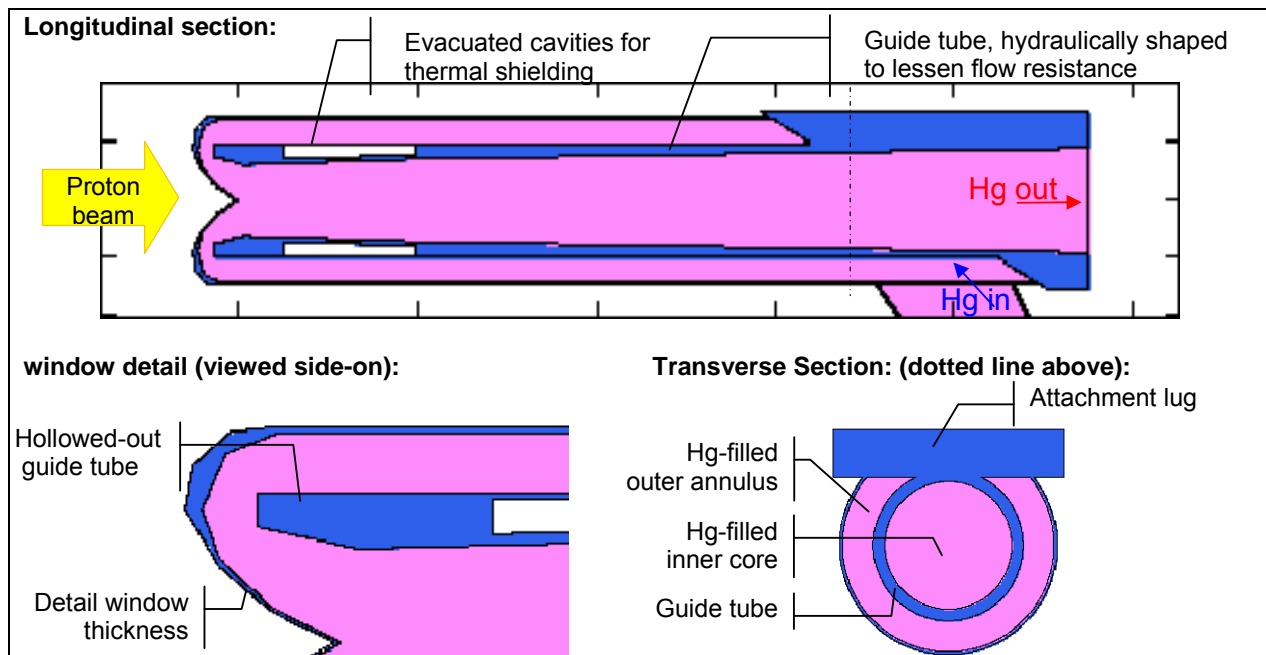
Figure 7: Detail FLUKA model for the base version of the neutron spallation target

The new target model is studied in isolation, without any ancillary equipment, surrounded only by a vacuum enclosed within an infinitely absorbing blackbody which captures all particles exiting the system. The profile of the beam impacting the target is a Gaussian; For the initial test, a normalised width σ = 2.5cm of the beam is chosen which is as wide as possible given that a Gaussian profile deposits 99% of its power over 3σ and the radius of the target is 7.5cm. A wider beam helps relieve heat deposition into the window and hence the stresses.

In order to test the model, the hollow steel guide tube is filled with mercury to verify whether similar results are obtained as in the concept study [Ref8], which has a simple 15 cm diameter steel container filled with mercury and no detail of the inner structure. The heat deposition, particle deposition, neutron flux, and spectra are extracted from the detail model of the base design and shown in the following pages. The neutron flux on the outer shell of the target reaches approximately 10^{14}[n/cm^2/s] per MW beam power as shown in Figure 8. In [Ref8] the calculation on a simplified full mercury target, albeit surrounded by a Beryllium Oxide reflector yields a similar neutron flux of the order of 10^{14} [n/cm^2/s].
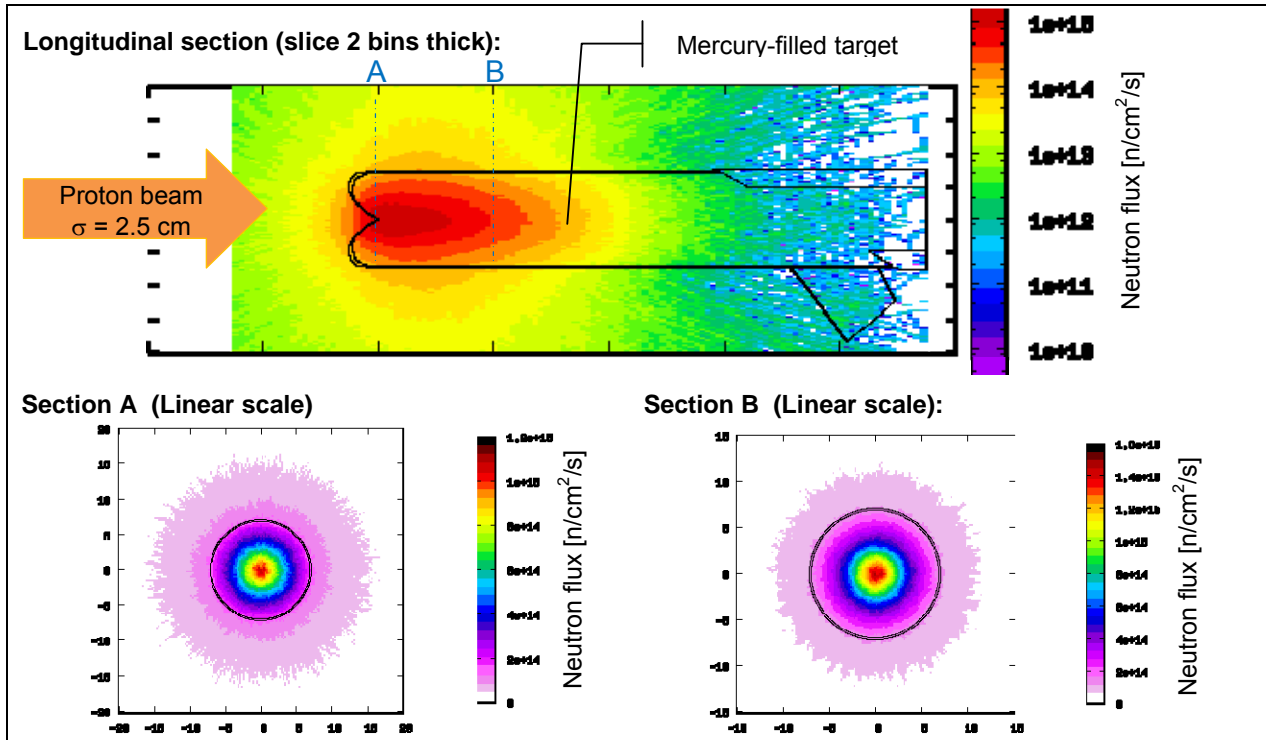
Figure 8: Maps of Neutron flux φ in n/cm²/s per MW beam power. Dimensions in cm.

Overall, the model filled with mercury agrees well with previous analyses. The energy spectra dn /d(lnE) of the neutrons escaping the targets is next examined in Figure 9; the lower left-hand graph and the detail in the middle graph show the difference between the spectrum averaged over the window and that averaged over the first 50 cm of the target. The forward end of the target is more productive in terms of flux and this is where a fission target should be placed. The middle graph shows the detail in the 100 MeV - 1 GeV band, it appears that the window spectrum is a little less energetic in the high energy band, due to the longer path from the central spallation zone. The right-hand graph in Figure 9 shows the evolution of the spectrum along the path of the exiting neutrons, by comparing spectra taken at the outer surface, at 4.9 cm and 3.5 cm from the beam axis, and normalising them at the 1 MeV peak. The gradual shift towards lower energies as the neutrons leave the central region is evident. These observations lead to the conclusion that affording exiting neutrons a shorter path through mercury should result in a harder spectrum which may benefit the production of isotopes.
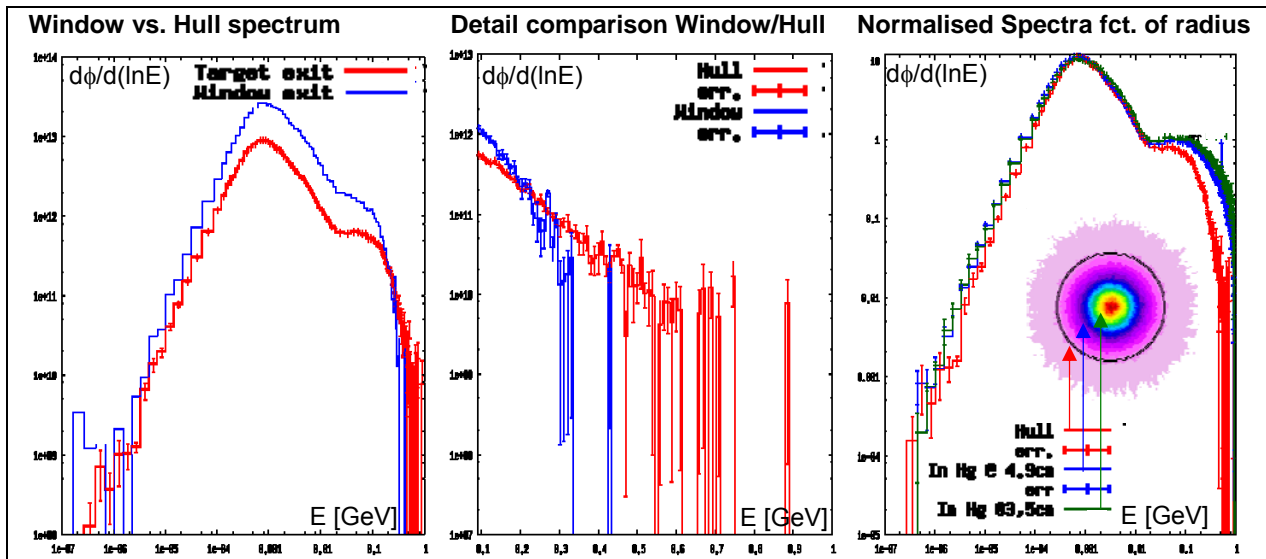
Figure 9: Neutron Spectrum dφ/d(lnE) . φ: Flux in n/cm²/s per MW beam power. E: Energy in [GeV]

A proposal for improving overall performance in relation to the isotope yield   15

4.2.2 Salient results from the base design

In a further development of the model (unchanged 15cm diameter), the guide steel tube with cavities is implemented and the effect calculated. Figure 10 shows the neutron flux resulting from this modification at the same scale as in Figure 8. The two distributions are quite similar. The flux exiting the hull on the surface is shown in the lower portion of Figure 10; the cylindrical outer hull is developed and the flux mapped thereon. It shows a peak located at the beam entry point of approximately 1.4 10^{14} [n/cm^2/s] per MW of beam power.
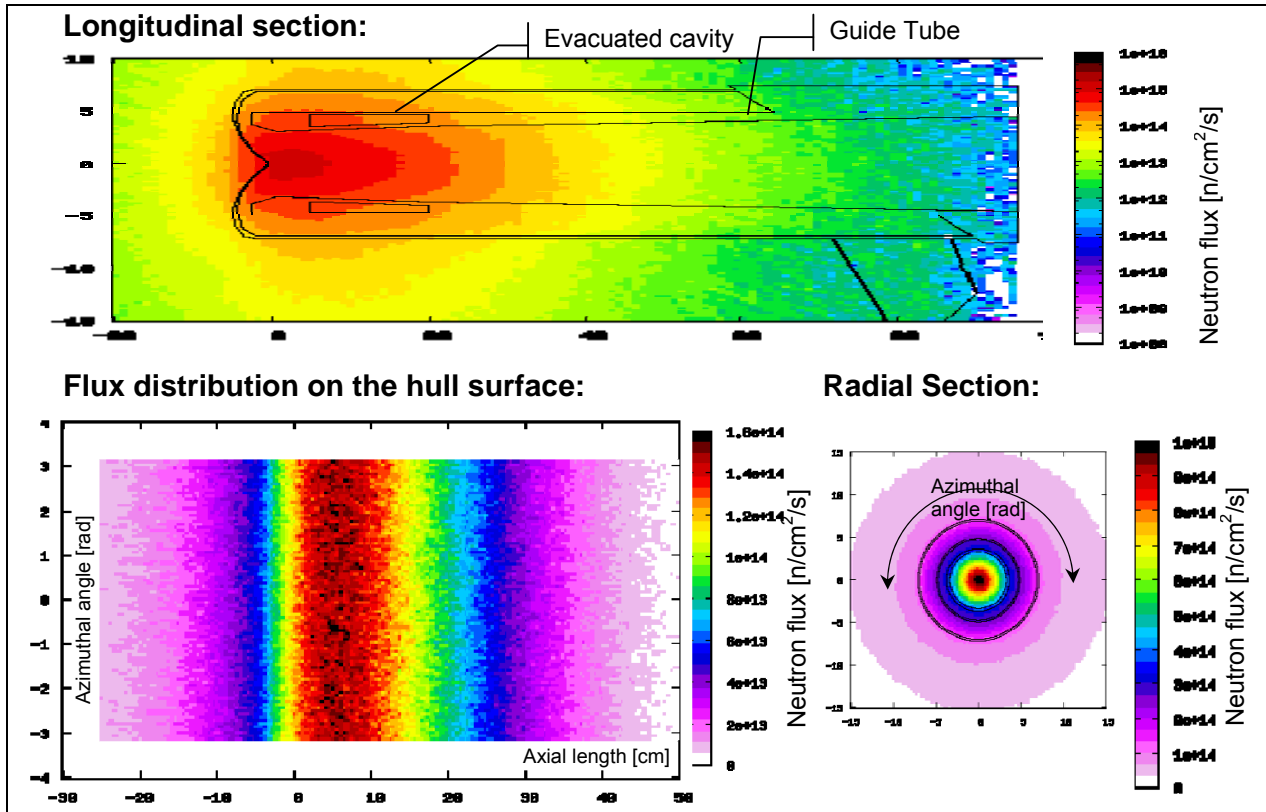
Figure 10: Neutron flux distribution per MW beam power.

The compared neutrons flux spectra in Figure 11 on the left, indicates a slight hardening of the neutron flux is brought about by the presence of a hollow guide tube. Note that in Figure 11, the spectrum of the flux ϕ [n/cm^2/s] is summed over the hull length and normalised for comparison purposes. The figure on the right also demonstrates a beneficial effect from changing the beam width, in terms of hardening the spectrum.

Figure 11: Normalised flux spectrum with vs. without guide tube (l.) and for various beam width (r.)

A proposal for improving overall performance in relation to the isotope yield   16

Next to the energy spectrum of the neutrons, the direction taken by the neutrons and the total number of neutrons produced per proton are also an important factor in selecting an appropriate design. The total production rate of neutrons, integrated over the entire hull surface and energy bands is examined in Figure 12 to check whether it matches established results on the production rates of neutrons by spallation. The neutrons are scored per incident proton. Figure 12 indicates a narrow beam narrow tends to produce slightly more neutrons and agrees well with results in [Ref8] which recorded 25 neutrons leaving the target per proton entering. Note that the σ definition for the Gaussian profile used in this report differs from that used in Fluka[*].

An interesting aspect of the neutron production rate is the fact that the model incorporating a guide tube captures a smaller proportion of neutrons on their way out of the target than the model filled with mercury; again an indication that the production of neutrons may benefit from designing a shorter escape route. Filling the target with mercury entirely does yield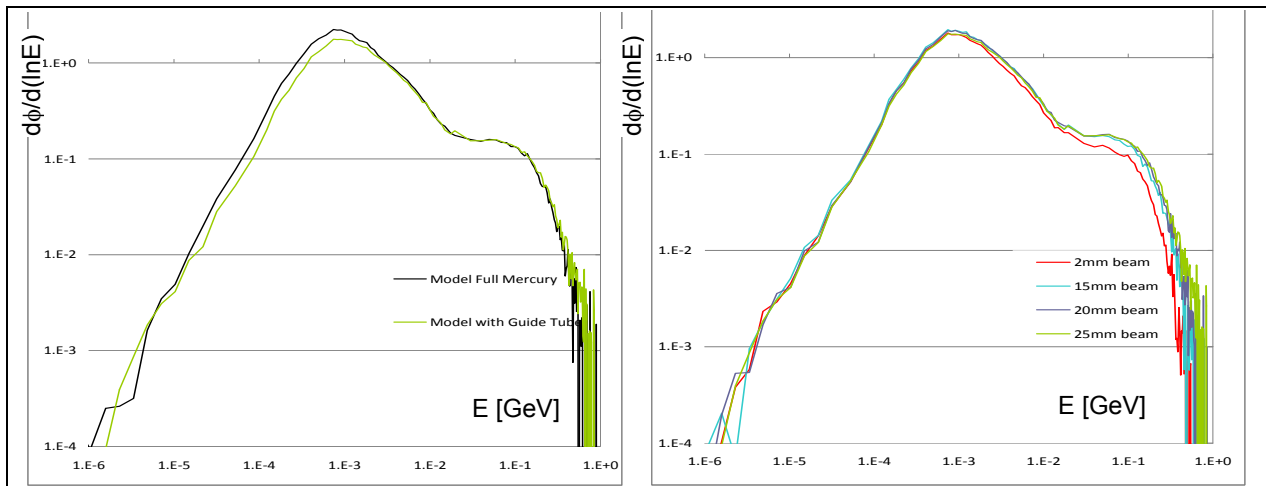 a greater number of neutrons simply due to the protons having a larger volume of mercury to impact; however the resulting neutrons occupy a lower energy band as demonstrated on the right of Figure 11.

[*] Beam width σ in [mm]	
Defined according to	
This report	FLUKA
$e^{-\left(\frac{r}{\sigma}\right)^2}$	$e^{-\frac{1}{2}\left(\frac{r}{\sigma}\right)^2}$
5	3.5
10	7.1
15	10.6
20	14.1
25	17.7
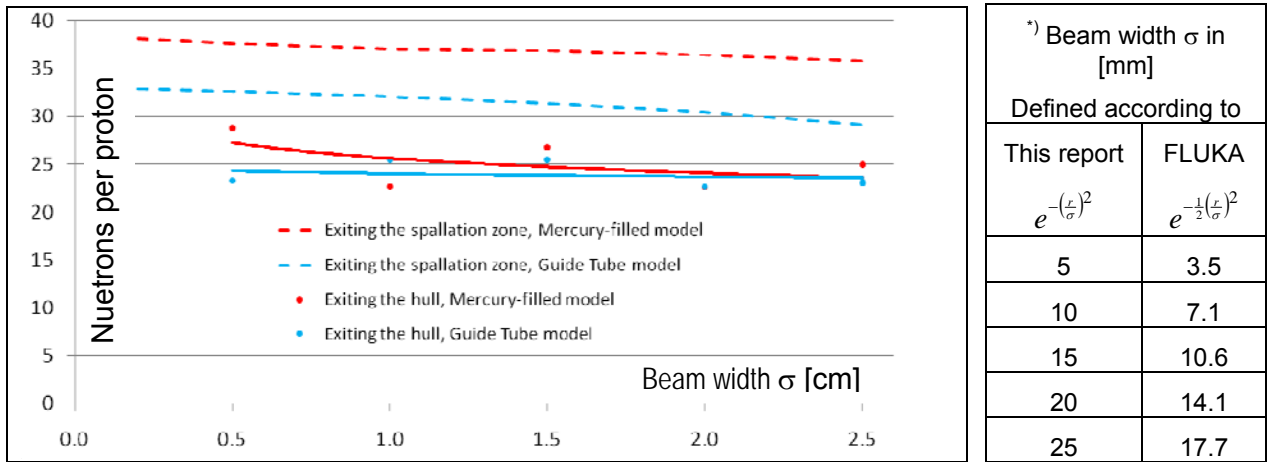
Figure 12: Neutron production rates according to the width of the beam

There are however some constraints related to the beam width, in particular shielding requirements and heat deposition limitations in the beam window. The distribution of charged particles shown in the lower portion of Figure 13 indicates a significant shower is emitted laterally into the guide tube for σ = 2.5cm, which precludes using too wide a beam. Admittedly, a larger beam does have an advantage in terms of lowering the heat deposition in the window. Figure 13 shows a beam width of 2.0cm limits the entry of beam particles into the guide tube and offers a reasonable compromise in terms of retaining a hard and dense neutron spectrum, whilst minimising the heat deposition of the proton beam on the beam window and the shielding requirements.
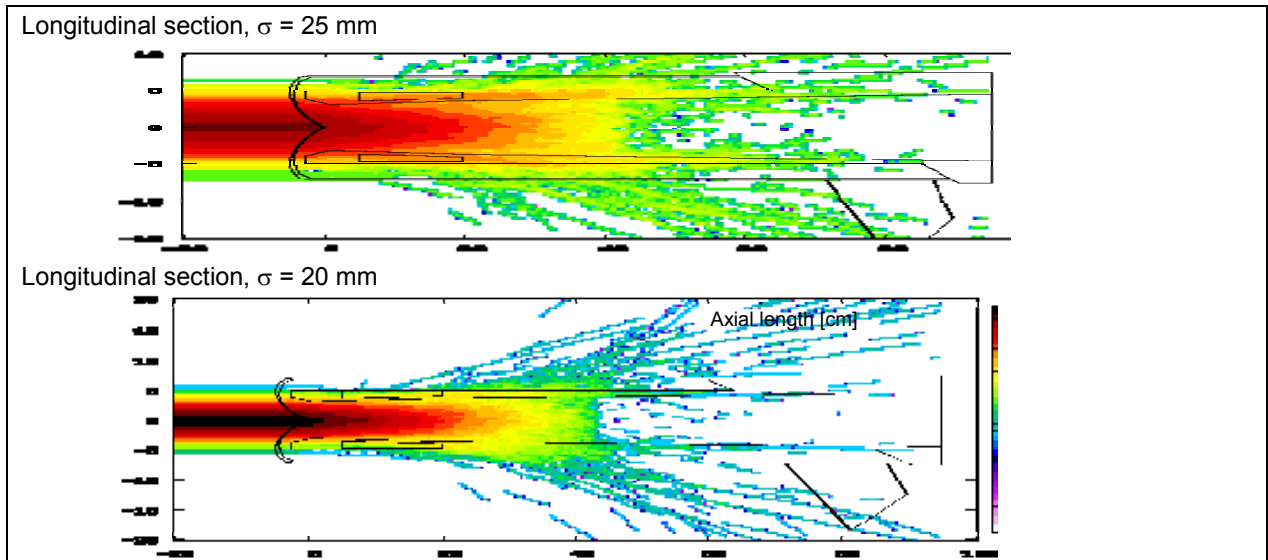
Figure 13: charged particles distribution for different beam widths

A proposal for improving overall performance in relation to the isotope yield

The distribution in terms of the direction of neutrons exiting the hull of the spallation target is shown in Figure 14, which gives the proportion of neutron flux according to solid angle cos(θ), where θ is the angle between the normal direction to the hull and the direction of the neutron path exiting the hull. Neutrons leaving the hull at an angle close to the normal direction account for 25% of the total flux. On the other hand neutrons leaving at a shallow angle below 26° barely amount to 1% of the total flux, and the high energy component at this shallow angle is virtually wiped out. The loss of energy for neutrons escaping at a shallow angle and the prevalence of the normal direction for the neutron flux are a logical consequence of the shorter route for neutrons escaping in radial direction from the central spallation region. It would therefore seem beneficial to encourage neutrons in the centre region to exit in radial direction so as to improve the density and spectral distribution of the flux in the high energy band.
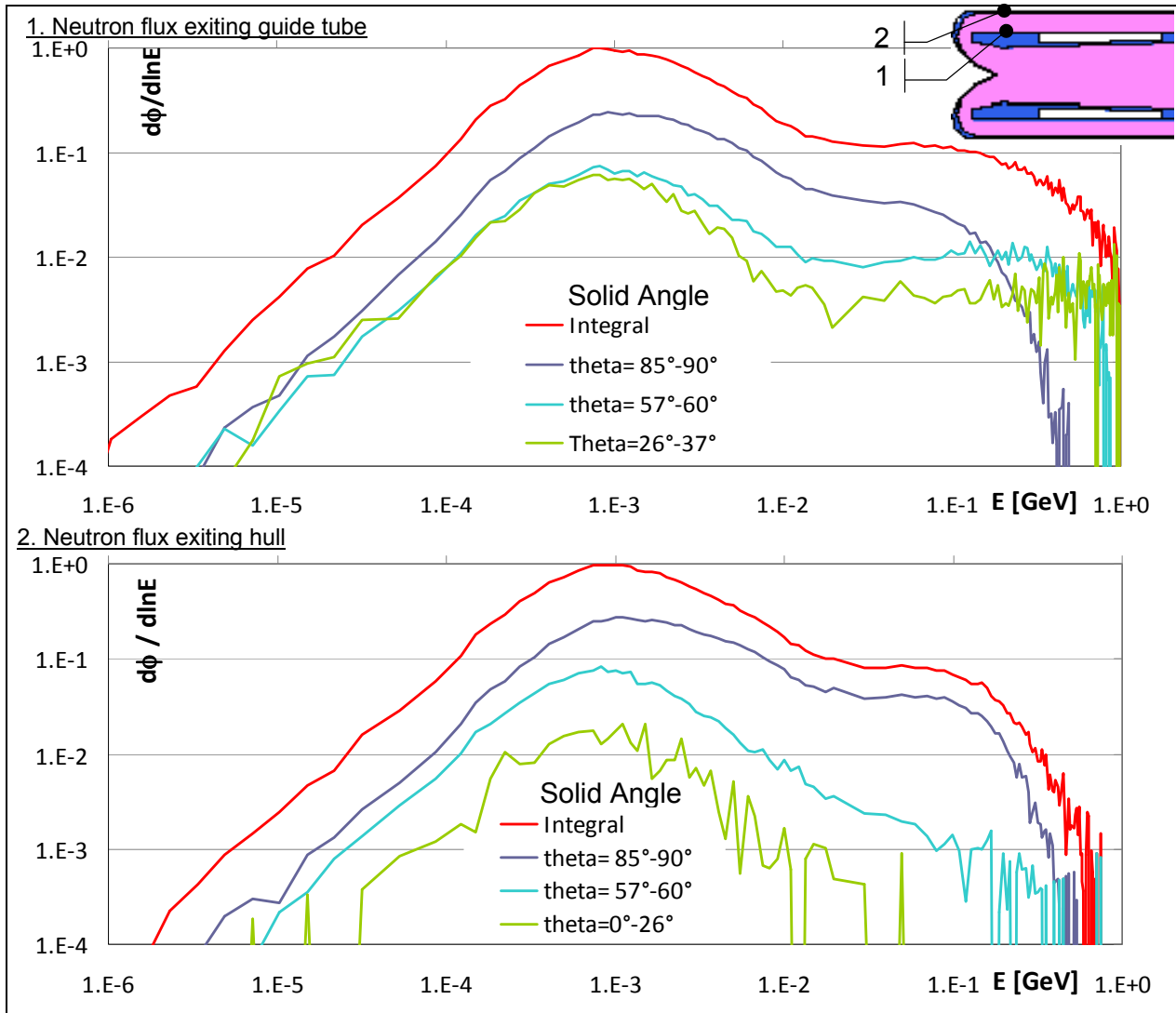
Figure 14: Neutron flux spectrum as a function of solid angle

The initial neutronic evaluation of the base design has hinted at possible improvements which will be examined in the following. These options can be briefly summed up as:

- Integrating a hollow guide tube should not only benefit the thermal-hydraulics, but also the proportion of neutrons escaping the hull

- Giving a more direct escape route to neutrons leaving the central spallation region by side wedges.

- Attempting to collimate the spallation neutrons in radial direction with respect to the beam axis, by integrating reflectors, both inside the neutron source and around it.

A proposal for improving overall performance in relation to the isotope yield   18

5 Evaluation of design improvements to the neutron source

The previous analyses have given some leads as to possible improvements benefiting both the hydraulic and neutronic aspects. The CFD analysis in [Ref.11] indicates that the major source of instability lies at the vertex of the beam window, a matter of concern which is currently dealt with using a flow reverser. As this item is complex and requires validation in a test, it seems the idea of increasing the incomer diameter would offer a better solution. The net effect of increasing the overall annular dimensions of the incomer is to increase the bending radius at the apex of the beam window thus making it easier for the flow to reverse 180°. Another idea for the neutronic study involves adding wedges in the incomer along the side of the source (ref. Figure 4). The wedges are located in a section where speeds are relatively low at around 1 m/s and could be easily increased. Their implementation should also help straighten the flow in the incomer, benefiting stability.

5.1 Incorporation of thickened guide tube and lateral "neutron windows"

The neutron source diameter will now be increased from 15cm to 19 cm with the aim of improving the hydraulic performance at the beam window. In addition to the diameter increase, there are two main design changes; the first is a thicker hollow guide tube as well as two vacuum-filled wedges in the outer annulus of the incoming mercury-filled channel (rf. Figure 4). In this manner it is hoped the flow of liquid metal into the beam area will be improved whilst affording neutrons a better chance of survival when leaving the spallation zone. The model developed in the previous section is therefore modified to incorporate the proposed wedges as depicted in Figure 15. In the following sections, the wedges will be designated "neutron windows"
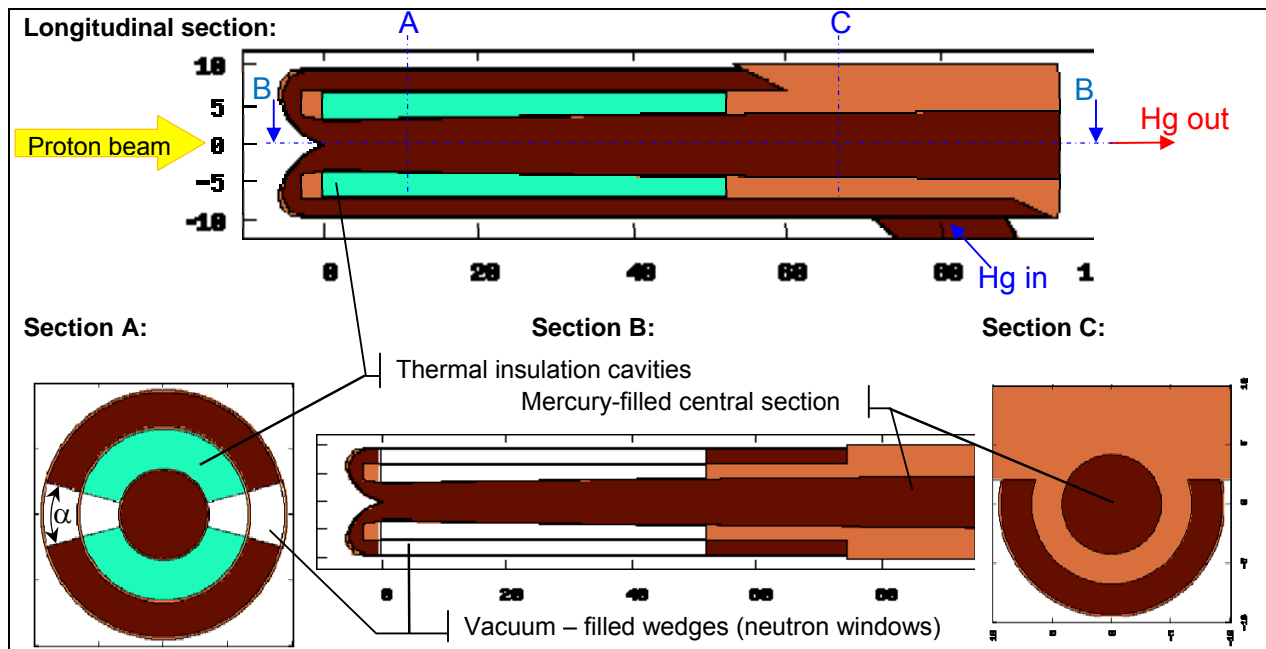
Figure 15: Detail model for suggested improvements of the neutron spallation target

The neutron windows can be varied in length and width. For hydraulic reasons it simpler to allow the neutron windows to run the full length of the incoming annulus as this separates the annular flow in two distinct channels. The angle however can be freely chosen, in a first iteration the opening angle is varied according:

α =   30°   45°   60°   90°

The neutron flux on the outer surface of the hull is plotted for these different angles as shown in Figure 16. The top left distribution shows the flux on the ø19cm hull for the version without windows, and peaks at

$1.2*10^{14}[n/cm^2/s]$. The flux at the exit of the ø15cm base design is $1.28*10^{14}[n/cm^2/s]$. The effect of the neutron windows is quite visible in the middle and lower portion of Figure 16, and demonstrates a local increase of the neutron flux to approximately $1.4*10^{14}[n/cm^2/s]$. As the window neutron angle opens, the area affected by the window increases as well, although the local flux peak decreases somewhat in relative terms. Overall the concentration effect on the neutron flux is quite marked and beneficial around the windows. There is a penalty however between neutrons windows as can be seen from the graph in Figure 16. The larger the windows the more the flux between windows tends to dip below the nominal flux for the base version (with no windows). These initial results show it is possible to increase the diameter of the hull from 15cm to 19cm, whilst obtaining locally a 15% increase in the neutron flux by using wedges.
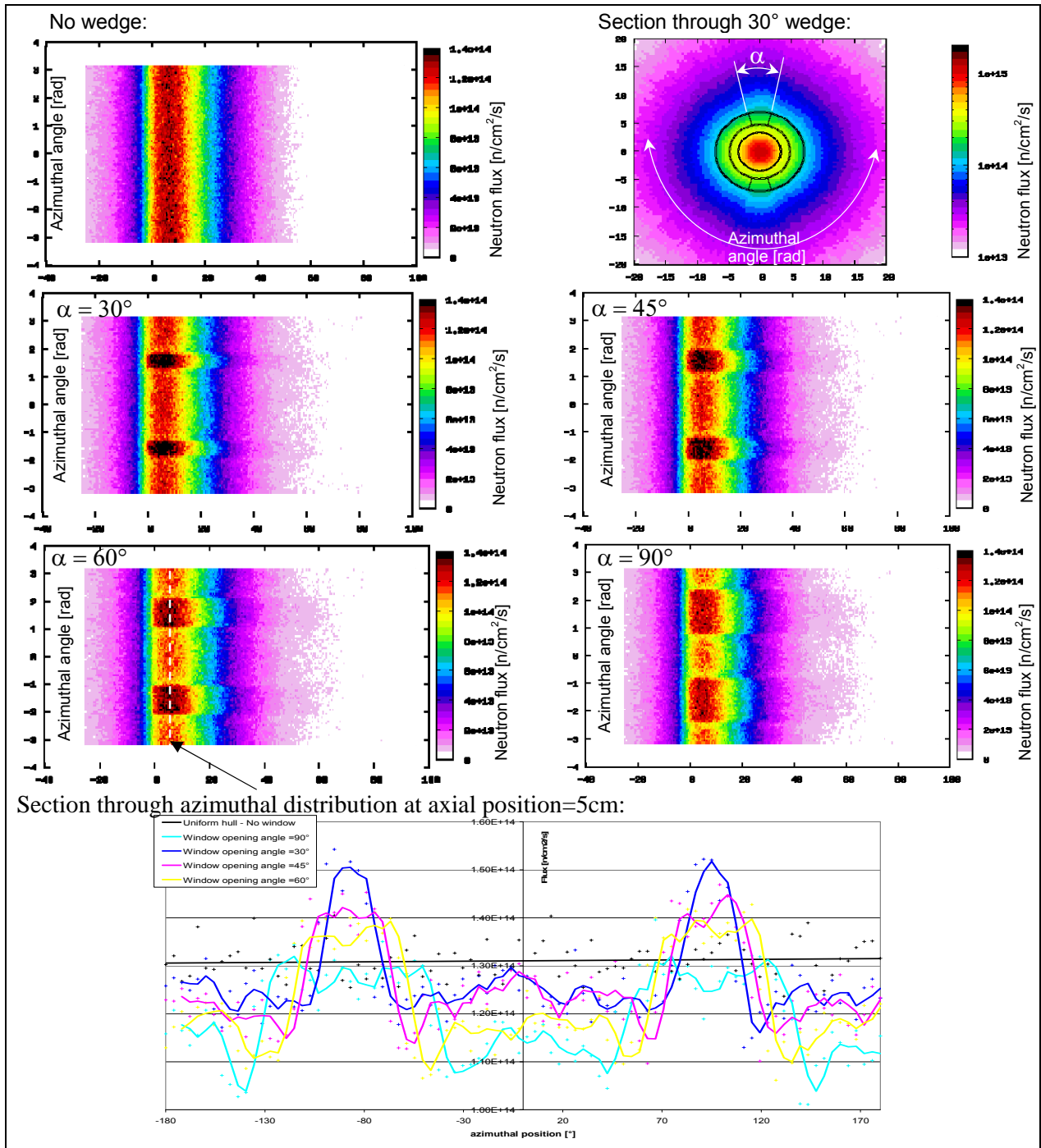

Figure 16: Neutron flux [n/cm2/s] per MW beam power for various opening angles of wedge
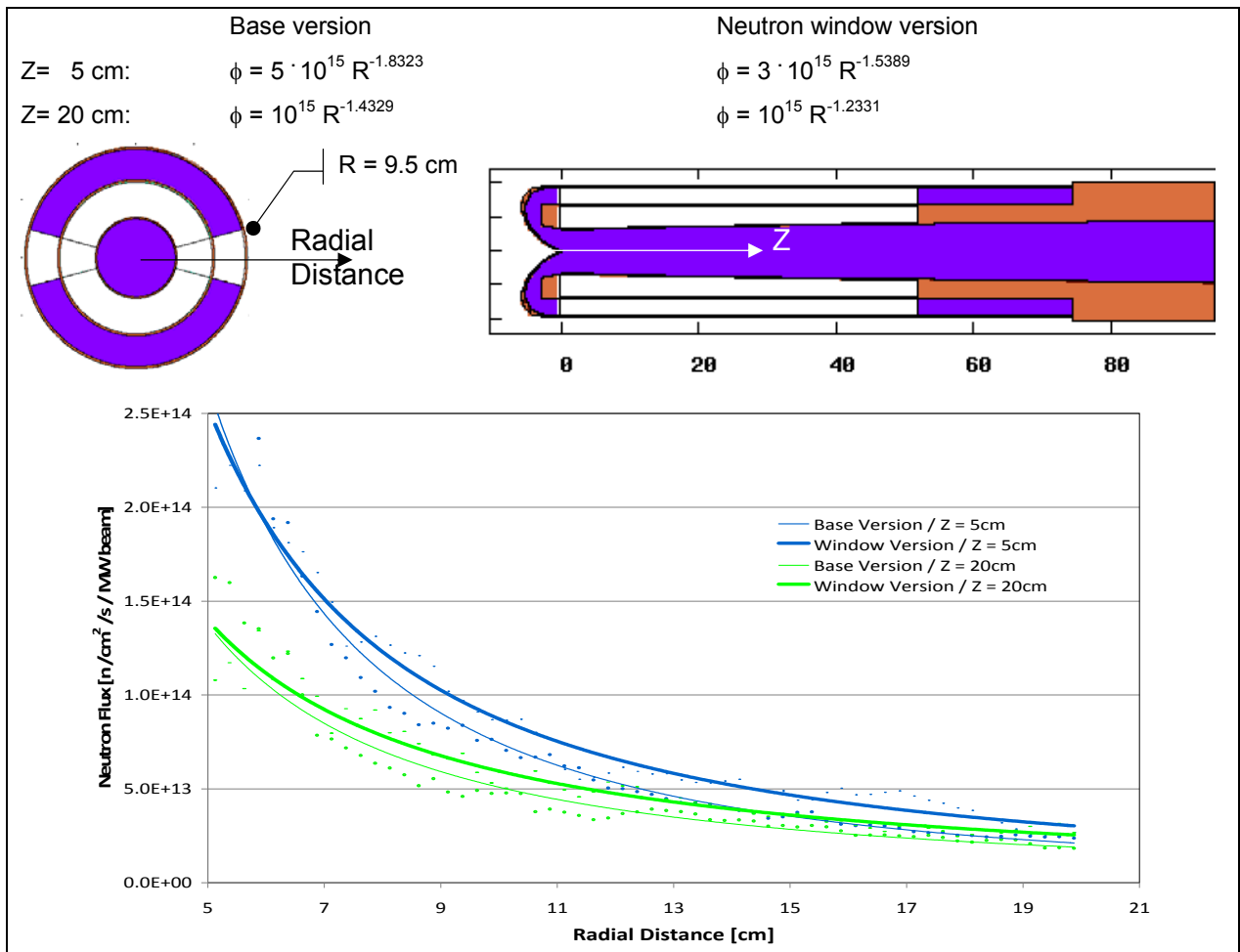
The following table recapitulates the neutron production in different areas per incoming proton. It appears there is an optimum at between 45° to 60°. For instance increasing the angle from 30° to 45°, a 50% increase in the neutron window area leads to a 44% increase in neutron production. On the other hand a 300% neutron window area increase from 30° to 90° results in a 250% increase in neutron production. The total number of neutrons exiting the hull is also slightly higher for 45-60° versus 90°.

Wedge angle	Neutron count per proton			
	1.Beside Neutron window	2.Neutron Window	Total ex hull 1+2	3. Ex Core
2 x 30°	17.75	4.37	22.15	25.05
2 x 45°	15.35	6.31	21.66	24.60
2 x 60°	13.11	8.02	21.13	24.26
2 x 90°	9.15	11.07	20.22	23.57
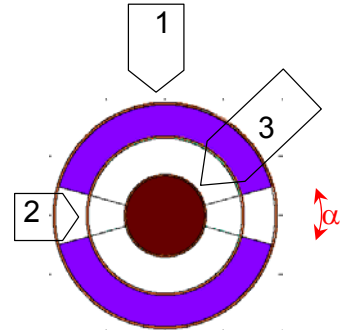
Table 4: Neutron production per incoming proton for various neutron window opening angle

The question of which angle is best in terms of neutron production cannot be dissociated from other aspects such as the spectral content which will be examined in the following. The neutron flux distribution in radial direction away from the central axis varies as shown below in Figure 17 for two stations along the beam axis. The base version follows approximately the $1/R^2$ rule, characteristic of a spherical distribution. On the other hand, the flux exiting the neutron windows tapers off more gradually, following an almost cylindrical distribution closer to $1/R$.

| Base version	Neutron window version
Z= 5 cm: $\phi = 5 \cdot 10^{15} R^{-1.8323}$	$\phi = 3 \cdot 10^{15} R^{-1.5389}$
Z= 20 cm: $\phi = 10^{15} R^{-1.4329}$	$\phi = 10^{15} R^{-1.2331}$

Figure 17: Neutron flux [n/cm2/s] per MW beam power away from beam axis

The increase in magnitude of the flux is accompanied by a change in the quality of the spectrum. A relative increase of the 100 MeV peak appears through the neutron window as compared to the rest of the hull. This effect is illustrated quite strongly in the spectrum, in Figure 18 hereafter.

The solid angles normal to the hull surface (Refer to curves for 85°-90° and 60°-66° in Figure 18) demonstrate most clearly the shift towards a harder spectrum in the neutron windows. Conversely the flux in the neutron windows decreases in hardness at shallow angles. The fact that the windows produce a harder flux perpendicular to the hull surface is consistent with the impression that the neutrons are more collimated as they exit the neutron windows. This effect could also account for the less rapid decrease in flux radially away from the source observed in Figure 17.

The overall outcome of modifying the guide tube seems to have the desired effect, i.e a locally more energetic and dense flux which should be beneficial towards creating a greater number of fissions in a target material comprising U238.
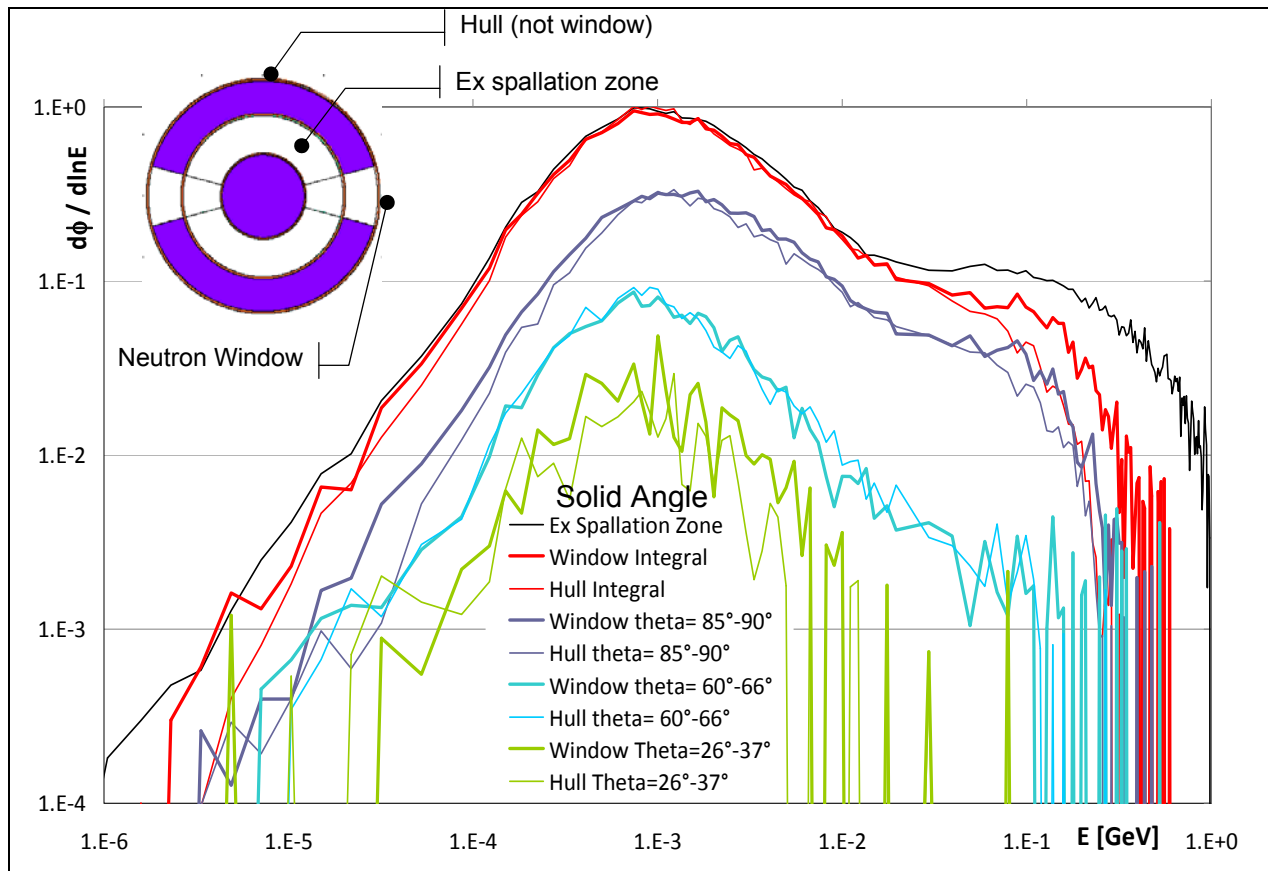
Figure 18: Neutron flux compared across the neutron window (bold) vs. in the rest of the hull.

The previous graph shows the spectral comparison for the point of maximum flux, roughly 5 cm from the origin, shown by a dotted line in the flux distribution in Figure 16. Although this position would appear at first glance, to be the most attractive for locating fission targets, the evolution of the spectrum along the length of the neutron source axis shows otherwise.

The change in spectral hardness along the beam axis is visible in Figure 19. The value of the neutron flux decreases along the axis, such that the different spectra peak at decreasing values. Hence, for a better assessment of the possible uses of the neutron flux, the spectra taken at different axial distances are normalised at the 1 MeV peak. It is thus possible to weigh up the relative proportion of neutrons in the second peak which is located at around 50 MeV.

Indeed, the harder part of the spectrum is of particular interest for fissioning U238. Although the net neutron flux decreases down the length of the source, the proportion of fast neutrons increases in relative terms. It

would therefore seem interesting to locate fission targets all along the axis, and not just at the point of peak flux (5cm from the origin at the beam window).

Of equal importance is the direction of the exiting neutrons. The spectrum for 30-50cm shows that a fair proportion of the hard spectrum between 100 MeV to 1 Gev is dominated by neutrons in the solid angle band from 0° and 35°. This is a limitation which will affect fission efficiency negatively, as neutrons which are not collimated in the direction of the fission targets are more likely to be captured in the surrounding structure.

The most effective locations for the fission target would therefore appear to be situated between -10 cm to +30cm along the beam axis, where the origin is the beam window tip.
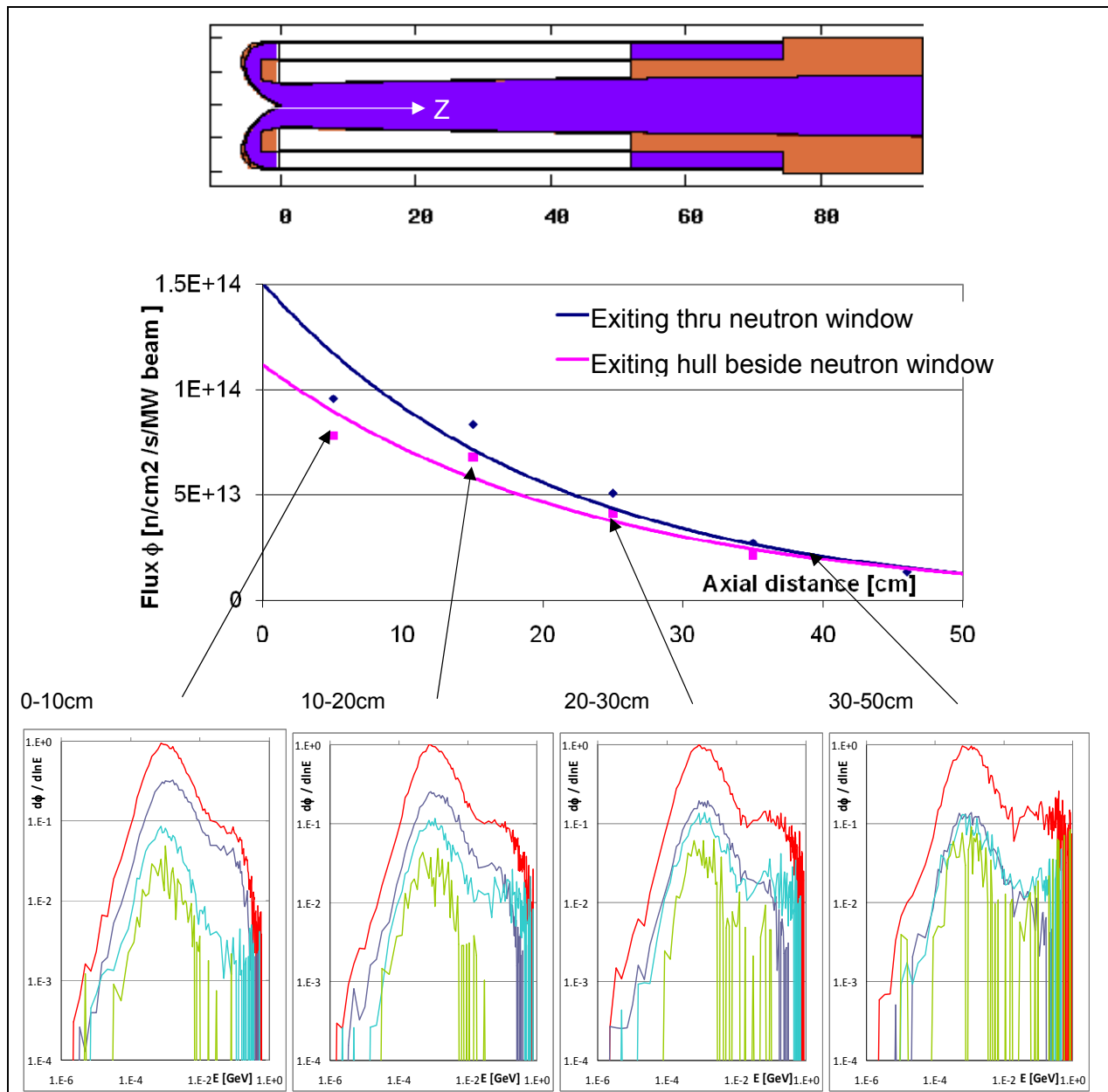
Figure 19: Neutron flux evolution across the neutron window along the axis.(scale as Fig.22)

The effect of changing the angle on the spectrum is negligible, the far greater influence being the axial evolution of the spectra shown in Figure 19. The neutron window wedge angle is therefore mainly linked to the peak fluence, whereas the spectrum is influenced by the overall neutron source configuration, such as the presence of a hollow guide tube, or (as in the next section) a reflector.

A proposal for improving overall performance in relation to the isotope yield   23

5.2 Modifications to the hollow guide tube

The guide tube is currently 2.5cm thick which allows the volume to be occupied by a material which may reflect part of the neutrons produced in the central spallation region. The material chosen for this design is Beryllium Oxide which has the additional advantage of resisting high temperatures.

The effect in terms of neutron production from implementing a beryllium oxide reflector inside the guide tube is summed up in Table 5 below. Again, as in the previous optimization, it appears that the maximum gain may be obtained from choosing an opening angle between 45° to 60°.

| Version		Neutron count per proton				
Wedge	Reflector	Beside window	Neutron Window	Increase %	Beam Window	Total ex hull
2 x 30°	N.A.	17.75	4.37		5.14	27.26
2 x 45°	N.A.	15.35	6.31		5.12	26.78
2 x 60°	N.A.	13.11	8.02		5.08	26.22
2 x 90°	N.A.	9.15	11.07		4.91	25.13
2 x 30°	In Guide tube	16.44	5.18	19	5.73	27.35
2 x 45°	In Guide tube	13.80	7.41	18	5.51	26.72
2 x 60°	In Guide tube	11.50	9.35	17	5.42	26.27
2 x 90°	In Guide tube	7.48	12.40	12	5.09	24.97
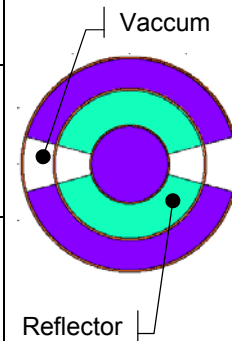
Table 5: Case study reflector optimisation with respect to neutron production

The effect of changing the reflector on the spectrum is negligible in the high energy band, there is a local increase below 1 MeV which could be of interest for fissile material, but has a negligible contribution for U238. The increase below 1 MeV concerns mostly solid angles below 60°, an indication that this increase is caused by additional interaction with the reflector.
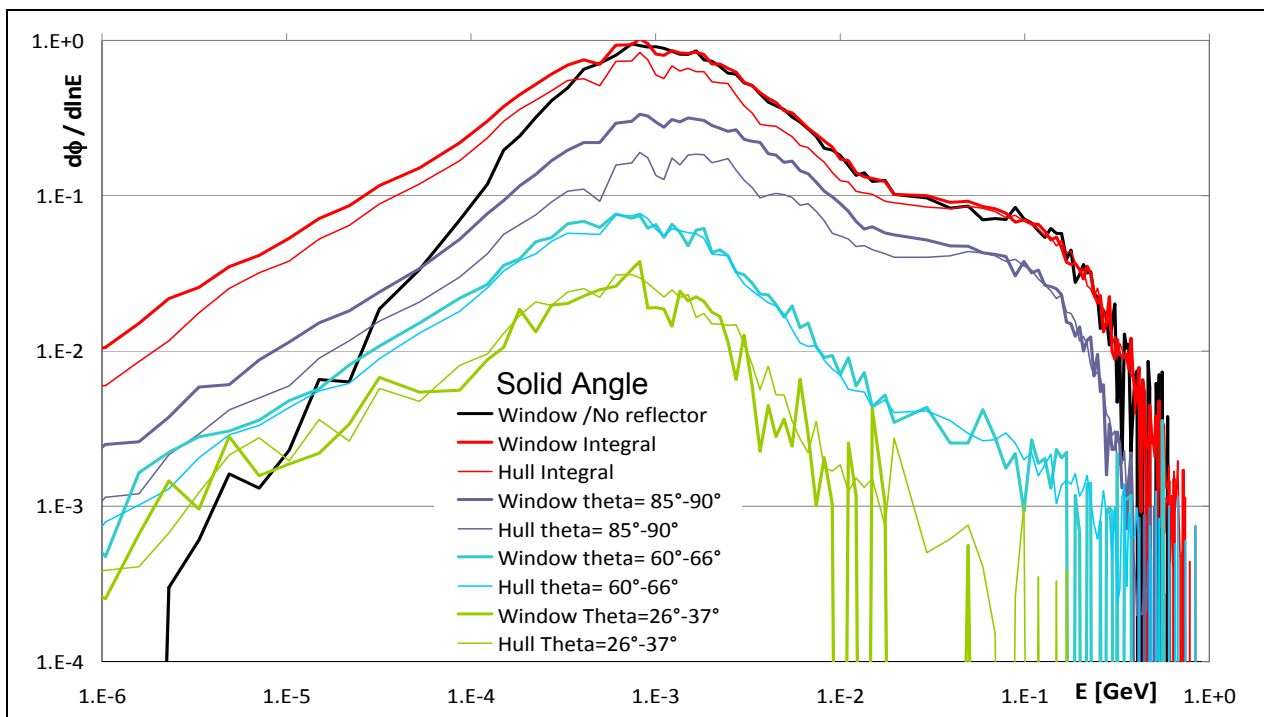
**Figure 20: Neutron flux modification due to the presence of a reflector**

A proposal for improving overall performance in relation to the isotope yield

5.3 Variation of the number of neutron windows

In view of the hydraulic results, it seems feasible to have a large number of wedges in the incomer to provide additional routes for the hard neutron spectrum such that additional fission targets may be placed in direct line-of-sight. A simple continuity rule links the velocity to the sectional area; it should be therefore possible to halve the sectional area of the incomer without adversely affecting the flow, which has a speed of 1 m/s in the base design. This entails the cumulated total angle of the wedges could reach 180°, which may be achieved either with:

-   one wedge up to 180°

-   two wedges up to 90°

-   three wedges up to 60°

-   four wedges up to 45°

These variations imply a change in the flow configuration which would have to be re-examined in detail as for the base design in section **Error! Reference source not found.** . This additional study will not be attempted within the scope of the current work; rather a qualitative assessment of the prior CFD results should suffice to gauge the ability of a specific design to deliver stable flow conditions. The net effect of these changes in configuration is assessed quantitatively by the tally of neutrons exiting the windows per incoming proton. The following figure shows the different wedge configurations which were calculated.
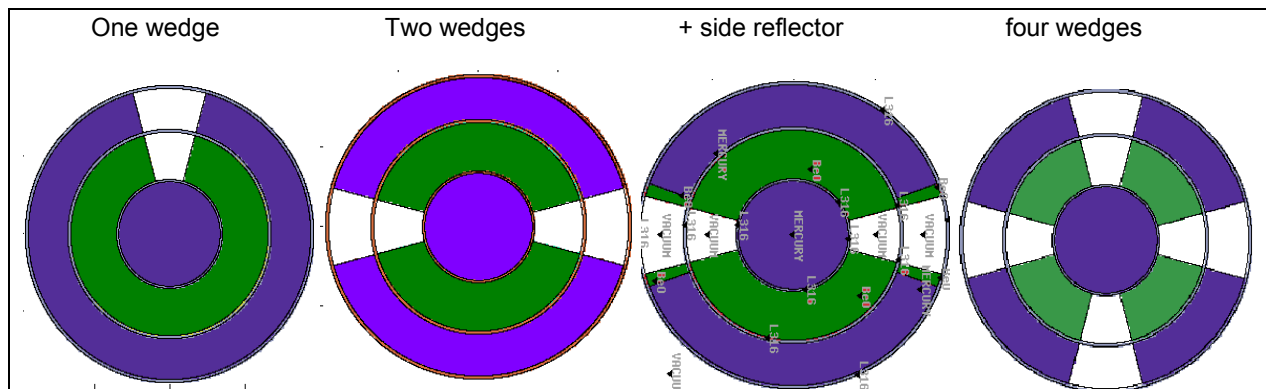
Figure 21: Configuration changes for the wedges and reflecting material

The first concept with a single wedge has the advantage of concentrating the entire neutron flux towards a single focal point which is of particular interest for a certain type of configuration of the fission targets in which the targets are located in 5m long tube extending downwards towards the source from a top shielding. This so-called MAFF design will be explained in more detail in the following section.

The two wedge option is the most advantageous from a hydraulic point of view, as it evens out the liquid metal flow entering form the lower off-centre inlet and thus helps ensure better stability downstream at the beam window.

The previous observation concerning collimation of the neutrons leads to the third design option in which reflector material is added to the sides of the wedges in an attempt to further direct the flow of neutrons outwards.

Finally the options with four wedges would at first glance appear rather complex, but it is simple enough form a manufacturing point of view and would essentially serve as a flow straightener in the incomer section of the source. There would be a slight penalty in terms of increased skin friction along the additional wetted surface, but the main contribution to the pressure drop lies in the beam target area which would remain unaffected by the change. The results are summed up in Table 6 hereafter.
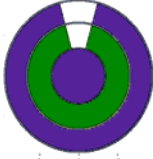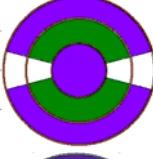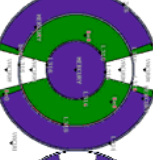
| Version | | Neutron count per proton | | | | In source |
| Wedge | Reflector | Exiting the hull | | | | |
		Beside Neutron window	Neutron Window	Beam Window	Total ex hull	Ex Core
1 x 30°	In Guide tube	17.39	4.46	5.88	27.73	35.64
1 x 45°	In Guide tube	15.14	6.58	5.77	27.50	34.48
1 x 60°	In Guide tube	12.93	8.51	5.74	27.18	33.41
1 x 90°	In Guide tube	9.04	11.94	5.53	26.51	31.61
2 x 30°	In Guide tube	16.44	5.18	5.73	27.35	33.40
2 x 45°	In Guide tube	13.80	7.41	5.51	26.72	31.24
2 x 60°	In Guide tube	11.50	9.35	5.42	26.27	29.68
2 x 90°	In Guide tube	7.48	12.40	5.09	24.97	26.90
2 x 30°	Along wedges	16.39	5.10	5.70	27.18	33.68
2 x 45°	Along wedges	13.79	7.39	5.59	26.76	31.49
2 x 60°	Along wedges	11.42	9.31	5.43	26.16	29.71
2 x 90°	Along wedges	5.94	12.11	5.15	23.20	26.77
4 x 30°	In Guide tube	11.64	9.26	5.40	26.31	29.68

Table 6: Neutron production per incoming proton for various wedge configurations

The efficiency of the one wedge version can be deducted from relating the neutron production to the total angular width of the wedges. For instance in the case of two 90° wedges, 12.4 neutrons exit the neutron windows, whereas with a single 90° wedge 11.94 neutrons are produced a 4 % reduction of neutrons for a 50% decrease in neutron window size. The resulting flux maps are shown below in Figure 22.
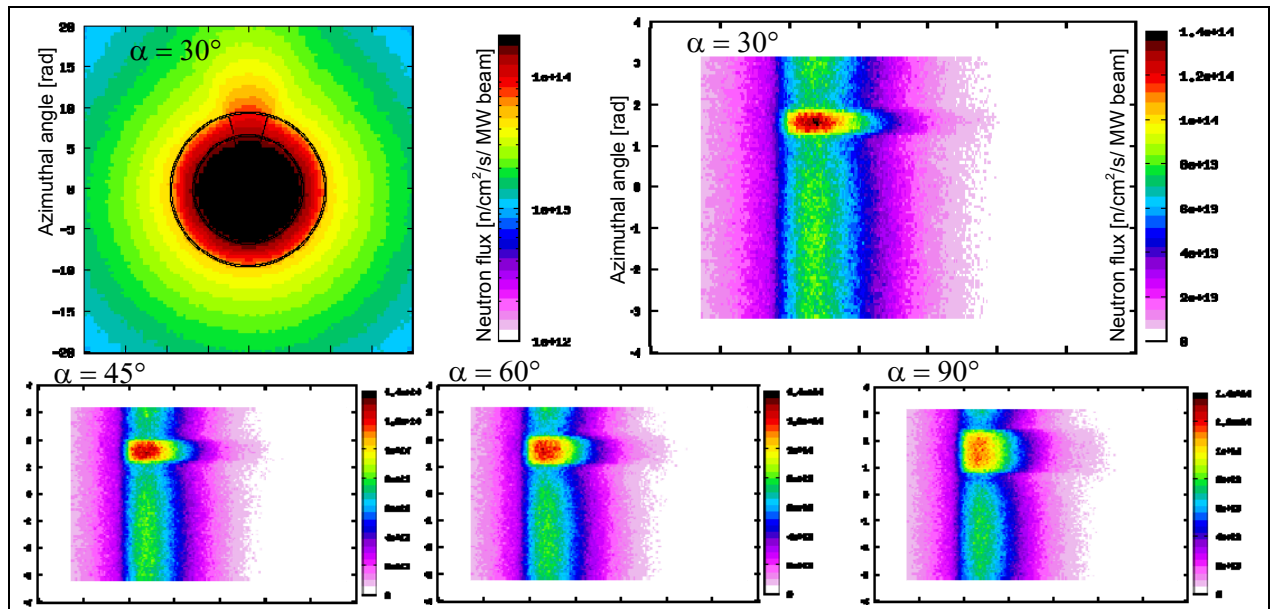

Figure 22: neutron flux density at the surface of the hull with one wedge

A proposal for improving overall performance in relation to the isotope yield

The version with one wedge has the best efficiency in terms of neutron production and may be retained in the future for the MAFF design. On the other hand, the compared production rates of the design with two wedges and the variant comprising reflector material along the opening angle of the wedges show very little difference. This is an option which will not be retained in the following optimisation study.

The option with four wedges has been analysed with an angle opening of 30°. A comparison with the two-wedge option shows that the production of neutrons is similar to that of two wedges at 60°, which have the same total width as four wedges at 30°. Therefore, in terms of neutron production the number of wedges can be increased at will without affecting the production of neutrons per unit width of beam window. This feature of the design with wedges entails that the placement of the windows can be optimised in relation to the desired position of the fission targets

Figure 23 shows the neutron density flux obtained with two or four wedges leads to a clear orientation of the neutrons in the direction of the neutron windows.
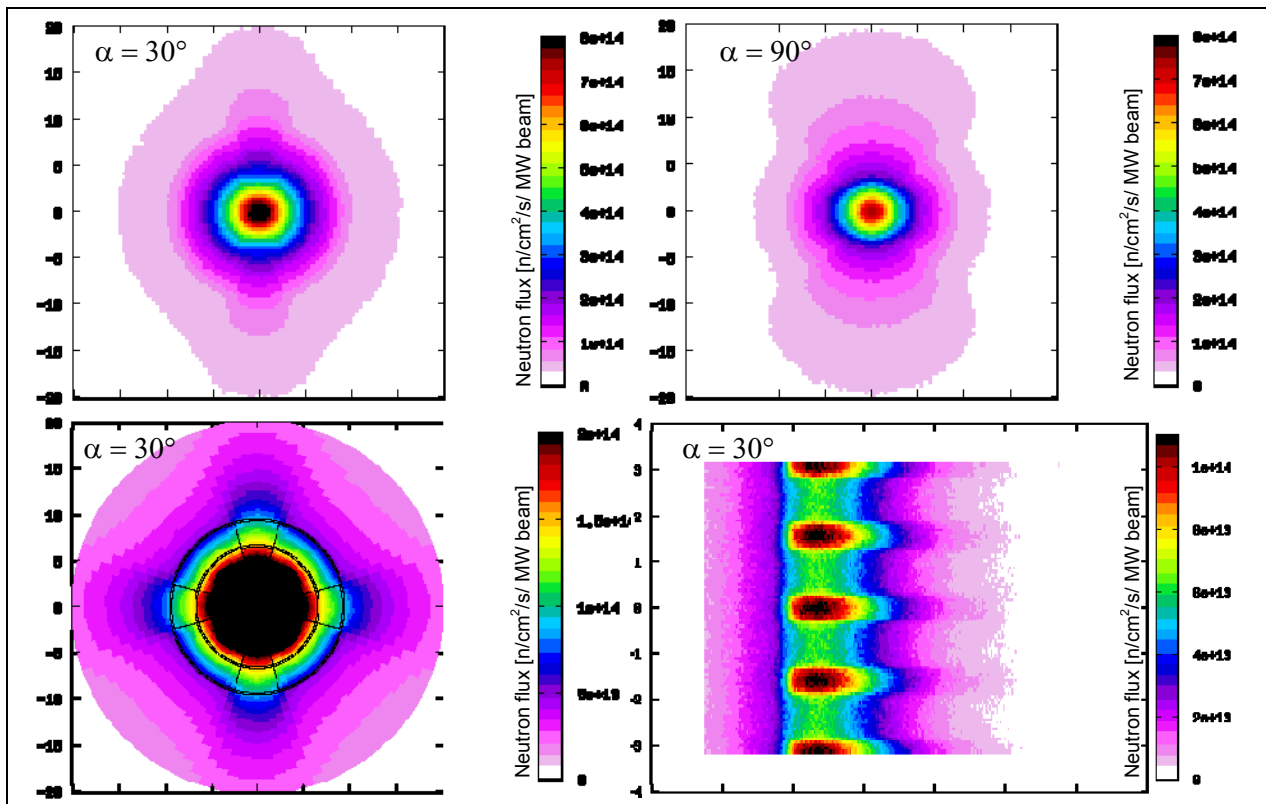
Figure 23: neutron flux density at the surface of the hull with two (top) and four (bottom) wedges

In terms of neutron spectrum, the shifts in hardness are similar to those observed in the previous section for the two wedges as explained in Figure 18, and which denotes a hardening around the second 50 MeV for the neutron flux exiting the neutron window.

The effect of implementing a hollow guide tube and evacuated wedges has clearly a beneficial effect on the flux, at least locally. Thus the next stage of the optimisation will examine the fission targets and how best to position them in relation to the neutron source.

6 Design and integration of the fission targets

6.1 Fission targets

The fission targets comprise 1mm thick wafers of Uranium Carbide separated by 0.1mm evacuated interstitial gaps (the UCx density is adapted to account for this geometry). This fissile material is exposed to a neutron flux which results in fission producing isotopes in the matrix of the uranium carbide. The isotopes then diffuse to the surface of the wafers helped by the high temperature of 2000°C at which the fission targets are held.

From the interstitial gaps the isotopes in gas form migrate through a process known as effusion until they are ionised by a laser. The laser can selectively ionise certain isotopes according to the chosen wavelength which can be tuned to excite electrons in the outermost layers of the desired isotope. The electrons are then released into an electron cloud leaving behind an ionised isotope gas which can be accelerated by an electric field.

The design of the fission targets has undergone several design cycles, two of which are shown below in Figure 24. The fission material is made up of thin wafers which have the dual purpose of enhancing the effusion of isotopes, and also facilitates the evacuation of heat through a combination of radiative and conductive heat transfer. A heat resistant graphite frame surrounds the fissile material wafers and provides a conductive path to an intermediate heat shield, made of Tantalum. This tantalum box is itself contained inside an aluminium double-walled structure which is actively cooled by water or helium.
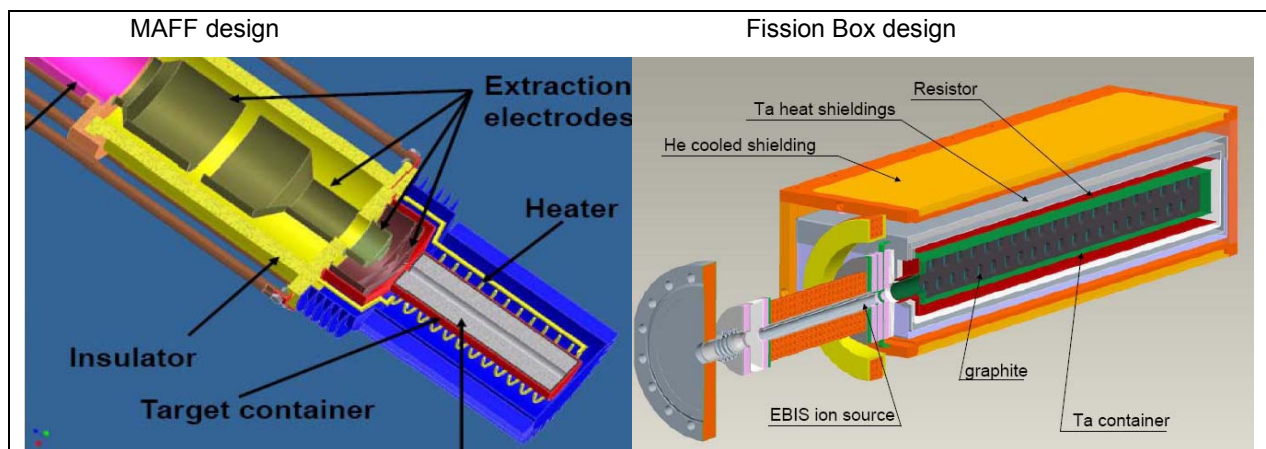

Figure 24: Two fission target designs [Ref10]

The laser used to ionise the gas is aimed centrally down the axis of the fission wafers which favours a design comprising a stack of uranium carbide wafers. Another possibility used in the Isolde facility is to aim a laser down a tube which interfaces with the side of the fission material stack. However this second option is considered less efficient.

The fission box comprises at it's outlet an ion source which serves to extract the isotopes through a high-voltage electric field in the order of several tens of kilovolts. For this reason, it is necessary to provide evacuated cavities around each successive shell to prevent arcing. A distance between shells of 1-2 cm is generally judged to be sufficient.

Accommodating the most favourable design for the ionisation of the isotopes leads to constraints which influence the position of the fission target relative to the neutron source. Indeed, it is necessary to include a space for the ion source and a beam tube coaxially with the fission material stack. The design is approximated as shown in the Fluka model below.
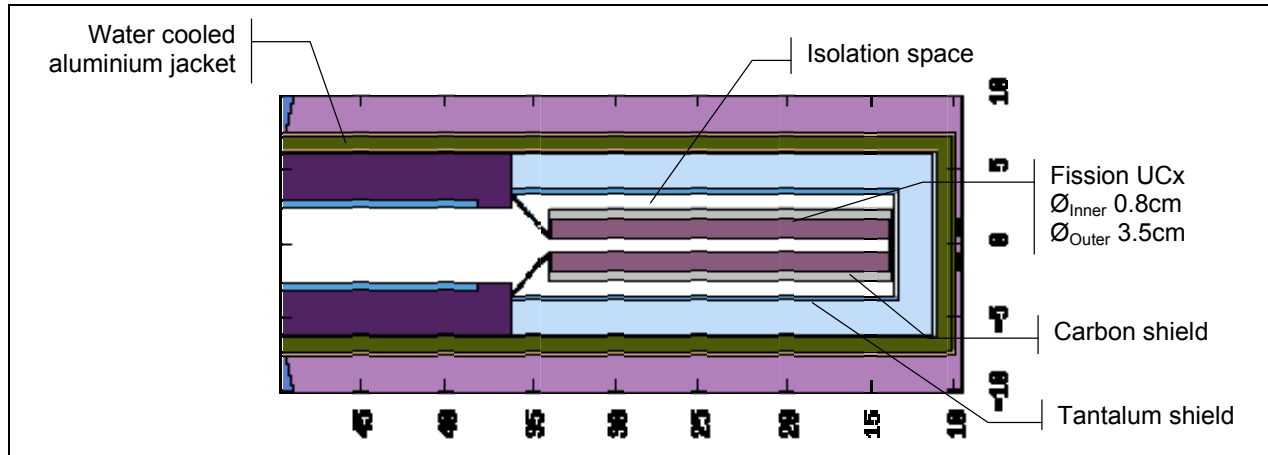
Figure 25: Fission target modelling in Fluka

6.2 Integration of the fission targets and source

There are two possibilities for integrating the fission targets with the converter source, the first shown in Figure 1 and the left of Figure 26 involves clustering the fission targets around the neutron source longitudinally. The second option inspired by the MAFF design of the Munich Institute of physics envisages 5 m long tubes extending downwards through a concrete shielding towards the target, as shown on the right of Figure 26.
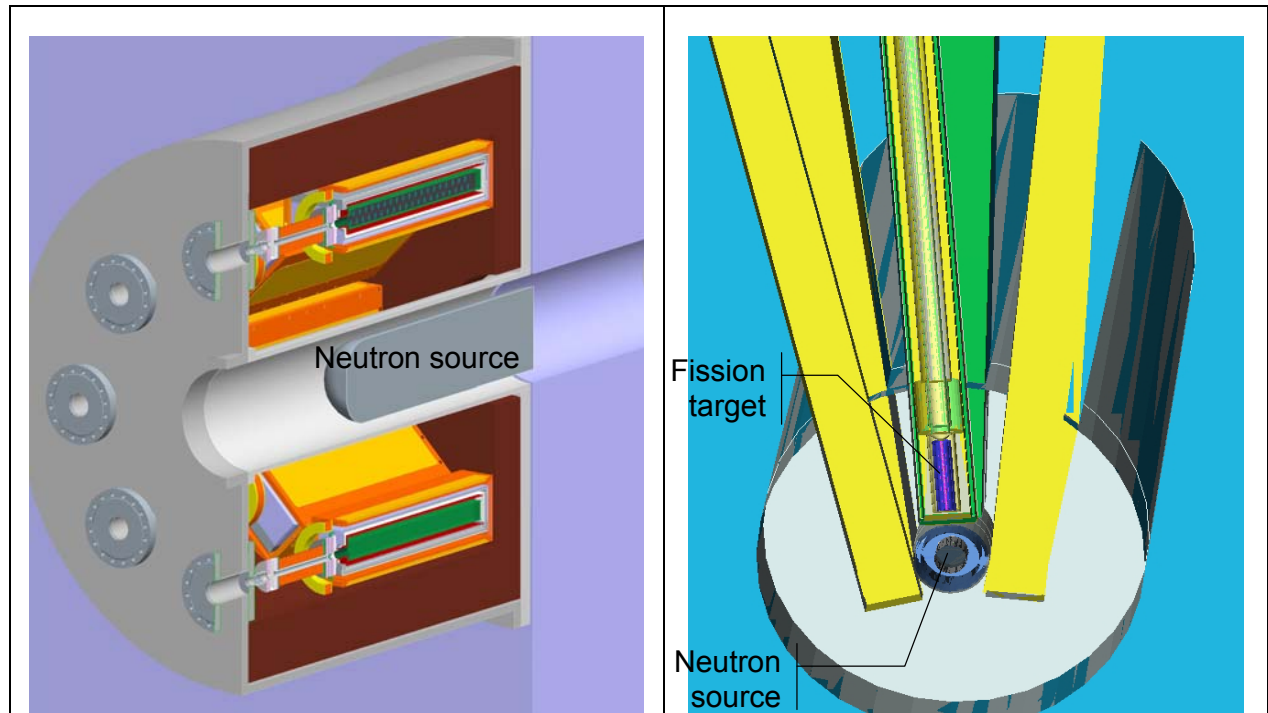

Figure 26: Fission target integration: radial cluster (left) and MAFF (right)

The two different possibilities will be examined in relation to the optimising position of the fission targets around the neutron source to increase the production of isotopes. The shielding calculations are not within the scope of the current study however.

7 Integrated Fluka model of the neutron source and fission targets

7.1 Integration of the models

The first series of calculations is aimed at verifying the interaction between the fission targets and neutron source, starting with a very simple configuration, in which four 4% enriched UCx fission targets cluster around a neutron source with four wedges. The neutron fluxes and overall fission levels are shown in Figure 27 below.

The fission density in the targets comes close to the goal set out in Table 1. However on a global scale, the number of fissions per second summed over 4 targets for a 4MW beam reaches 10^{15}, at the low end of the objectives (Table 2), which indicates the need for further optimisation of the disposition of the targets. The comparison normalised at the 1MeV peak in the top left-hand corner of Figure 27 shows the spectral evolution from the outer water jacket (blue curve) through the graphite (black curve) to the inner core of the fission material (orange & red curve). Clearly the neutrons in the epithermal region are absorbed in the outermost structure by the graphite and the water, before being finally absorbed by the U235. On the other side of the 1 MeV peak, the flux remains hard, as the structure does not impede significantly neutrons in this energy band. From 1 MeV to 10 MeV the fissile material does not absorb any flux, only around the 30 MeV peak does an absorption appear, which is likely caused by the U238, as the cross-section for fast neutron capture increase markedly after 10 MeV (Figure 28).
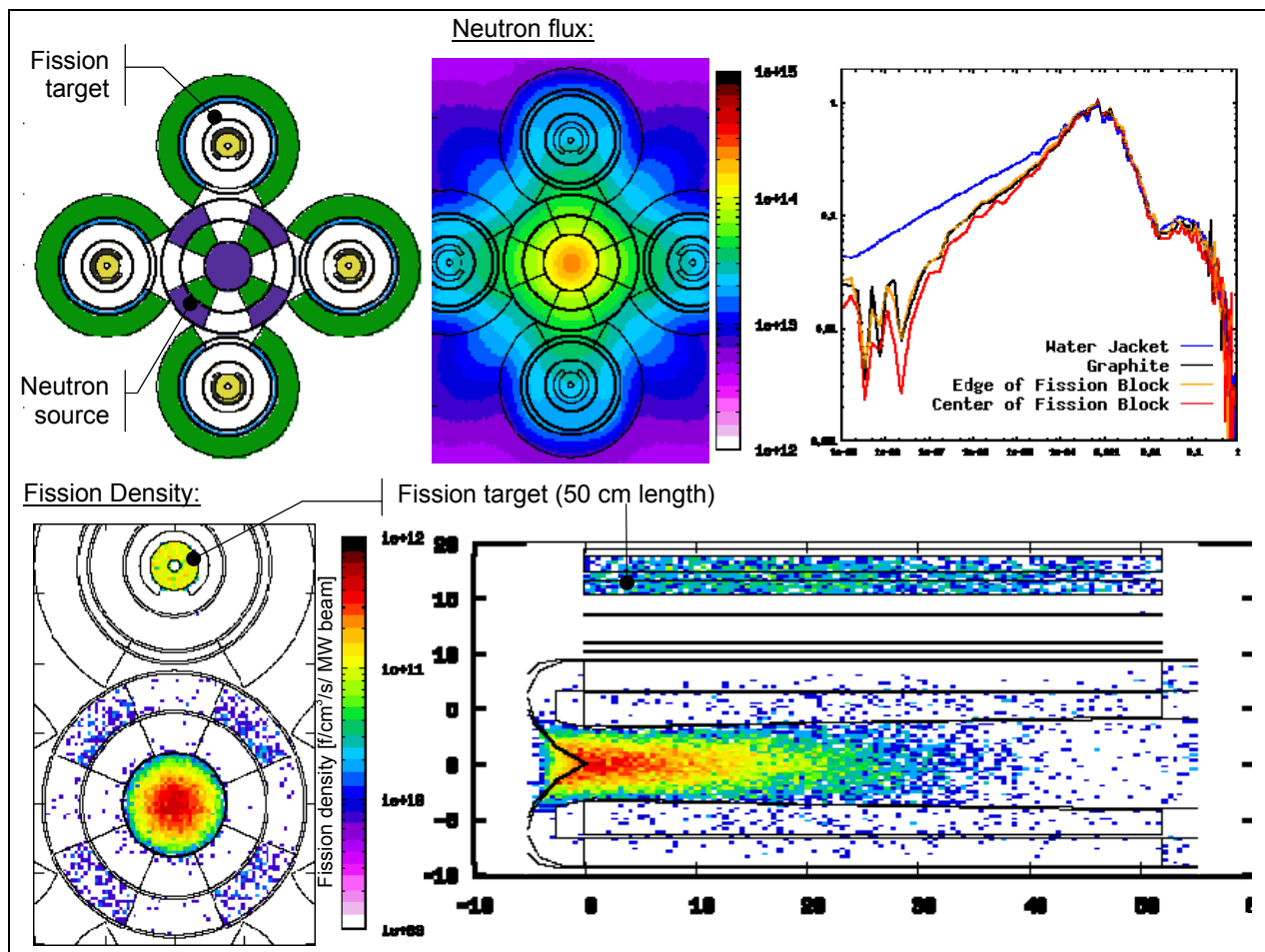

Figure 27: Neutron flux (top) and fission density (bottom) for a 4x fission target design per MW beam.
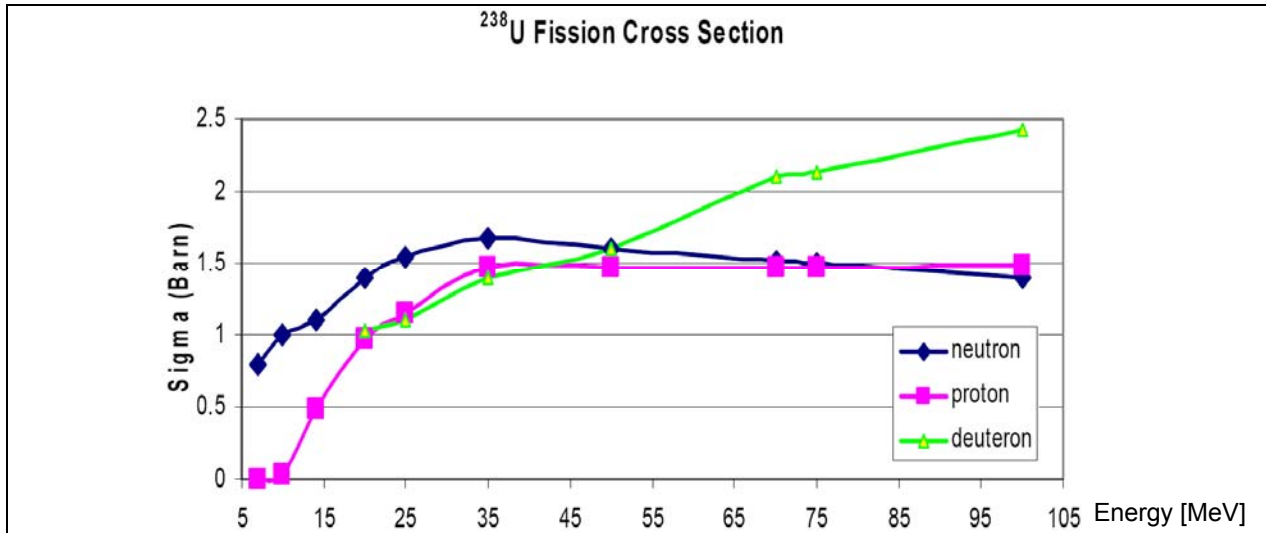
Figure 28: Fission cross-section of U238 in the rapid spectrum.

7.2 Optimisation of the target configuration

7.2.1 Implementation of a reflector

The possibility of integrating a reflector around the system to further enhance fission is next examined. A 200cm diameter cylinder is placed around the neutron source and fission targets and various reflector materials are tested. The table below shows the effect in terms of total fissions for a 4 MW beams.

Beryllium Oxide comes out as a clear success; there are however some technological constraints which may limit the use of this material in such great dimensions, such that the final configuration would probably a combination of beryllium for an inner cylinder and water in an outer surrounding jacket.

| Configuration | Fission Target | | | Reflector | Fissions per proton | 10^{15} Fissions @ 4 MW |
	Total length [cm]	Diameter [cm]	Total Volume [cm^3]			
Nominal	208	3.5	1897	Vacuum	0.038	1.0
Nominal	208	3.5	1897	BeO	0.240	6.0
Nominal	208	3.5	1897	Iron	0.102	2.5
Nominal	208	3.5	1897	Carbon	0.173	4.3
Nominal	208	3.5	1897	Water	0.188	4.7

Table 7: Neutron production for various reflector materials

7.2.2 Longitudinal position and shape of the fission targets

The fission density map in Figure 27 tapers off towards the end of the beam; the fission density is very much reduced after 30 cm. It would therefore seem profitable to shift the position of the fission targets in the direction of the fore end of the neutron source, but without changing the length of the fission targets (50cm each) or their diameter (3.5 cm).

The resulting effect in terms of total fissions is dramatic. Compared to the design with a reflector in place and four 50cm long / 3.5cm∅ targets in their original position, the 10cm position forward shift results in a 250% increase in the number of fissions; a sure indication that the new location is optimal.

A further attempt at improving fissions is to make the targets more compact, cutting their length in half and increasing the outer diameter from 3.5cm to 5cm, in such a way that the total volume of UCx remains unchanged. By concentrating ore fissile material in the optimal position, an increase of fissions is again achieved, this time by another 30%. Overall situating fissile material in the optimal position has tripled the number of fissions.

This last design is tested in combination with more realistic representation of the reflector, in which the previous 200 cm diameter beryllium reflector is replaced with a 60cm cylinder surrounded by another 40 cm of water. The net effect is to decrease the number of fissions by 18%, a penalty which may be worth the additional flexibility it offers in the design of the cooling system.

In a further attempt at optimisation, the fission targets are rotated 90° with respect to the beam axis; instead of lying parallel to the beam axis, the fission target axis points away from the source in radial direction. This proves to be the least favourable position, and produces a sharp reduction in the number of fissions. Although the rotated position is the preferred option for the MAFF design (ref. Figure 26), it would seem more opportune to keep the fission targets axis in the original position parallel to the neutron source axis. The isotopes could effuse sideways form the wafer in a manner similar to the experimented in the Isolde facility. Alternately, if locating a laser coaxially with the fission target is seen as essential, it may be possible to locate the ionisation laser in a fixed chamber, separate from the fission target block, whereby the fixed laser would interface with the fission target at the bottom of the MAFF beam tube through a laser-transparent window.
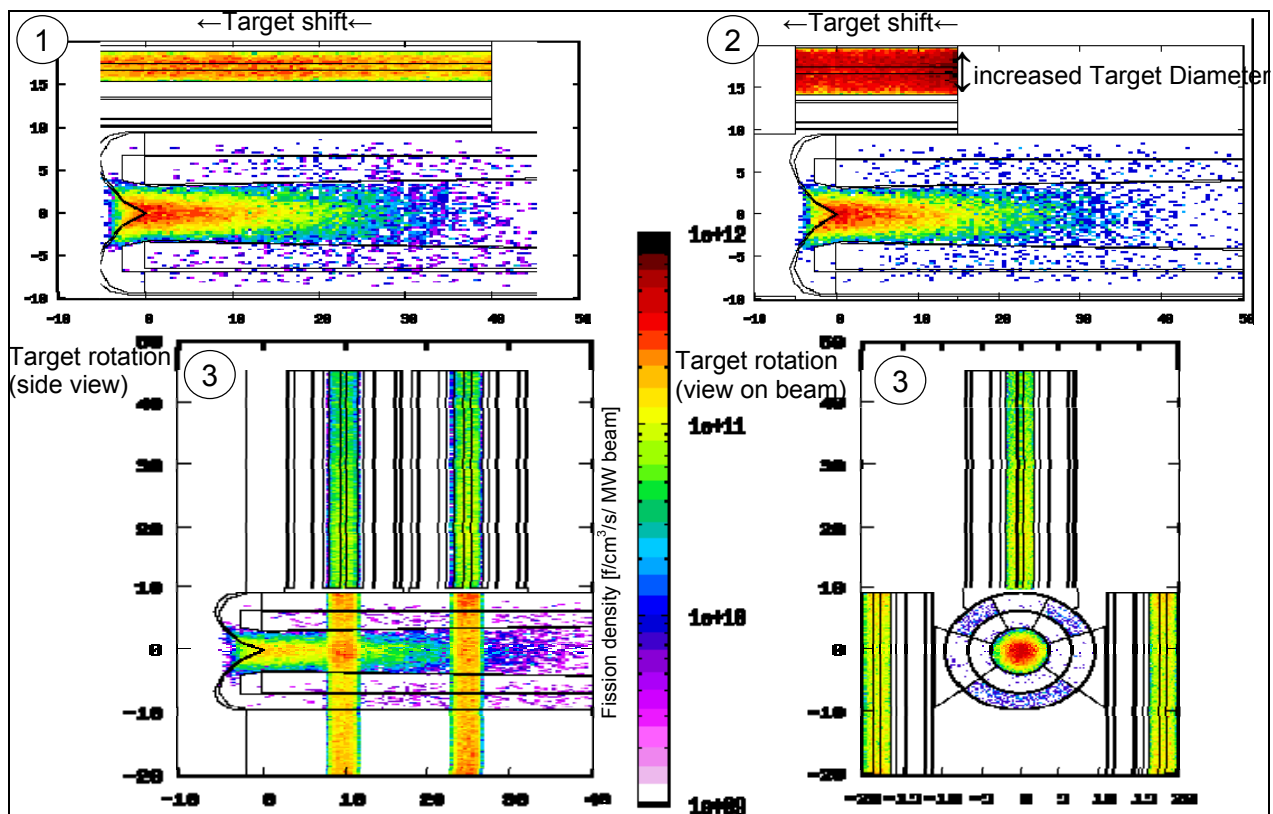

Figure 29: Fission density for three different fission target positions; ① thru ③ per MW beam power.

A compromise solution between the requirements for the MAFF design and those for the radial cluster may be a three wedge design which would allow MAFF type tubes to extend downwards from the shielding to all three positions around the neutron source, which would otherwise be more difficult with four wedges. The net effect is again to reduce the number of fissions however not significantly given the error margin.

| Refer. Fig.33 | Fission Target | | | | Nr. | Reflector | Fissions per proton | 10^{15} Fissions @ 4 MW |
	Configuration	length [cm]	Diam. [cm]	Total Volume [cm^3]				
1	Target shifted forward 10cm	208	3.5	1897	4	200cm BeO	0.524	13.0
2	Target shifted forward 10cm	104	5	1897	4	200cm BeO	0.662	16.5
3	Target axis rotated 90°	208	3.5	1897	3	200cm BeO	0.285	7.1
	Target shifted forward 10cm	104	5	1897	4	60cmBeO / 100cm H20	0.548	13.6
	Three wedge design	104	5	1897	3	60cmBeO / 100cm H20	0.534	13.3

Table 8: Dependence of the total neutron production on the position of the fission target

7.2.3 Radial position of the fission target

Finally, the restriction concerning the radial distance of the fission targets to the neutron source is examined in more detail. From an operational point of view, locating the fission targets very close to the converter does impose penalties on the design. In order to give greater allowance for ancillary equipment such as cabling feeder pipes and cooling it would appear necessary to free up this design constraint by moving the fission target radially outwards. The result of moving the fission targets radially is presented in Figure 30 and Table 9 below; there is no great change in the total number of fissions, as the variation is around 10%, which is within the numerical uncertainty. It therefore appears feasible to move the fission targets radially in line with the neutron windows and keep the flux relatively equal in magnitude.
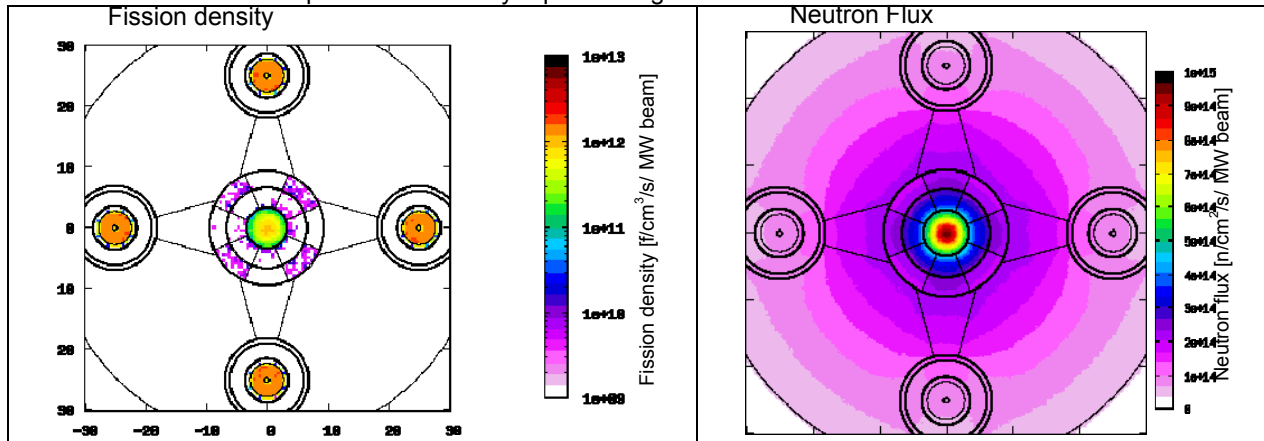
Figure 30: Fission density and neutron flux (per MW beam) for changed fission target radial position.

| Fission Target | | | | Reflector | Fissions per proton | 10^{15} Fissions @ 4 MW |
Configuration	Total length [cm]	Diameter [cm]	Total Volume [cm^3]			
In original radial position	104	5	1897	60cm BeO / 100cm H2O	0.548	13.6
Target shifted radially 3cm	104	5	1897		0.532	13.2
Target shifted radially 8cm	104	5	1897		0.464	11.5

Table 9: Total neutron production for various fission target location

A proposal for improving overall performance in relation to the isotope yield

8 Isotope yield of the fission targets

The neutron source and fission target chosen for the final study is shown in the figure below, and corresponds to the optimum position in the study detailed in Table 9 above.

The results computed here above all used 4% enriched uranium in the fission targets; for comparison it is interesting to examine the isotope yield not only with this material but also with 0.7% U^5 natural uranium which is more readily accessible.
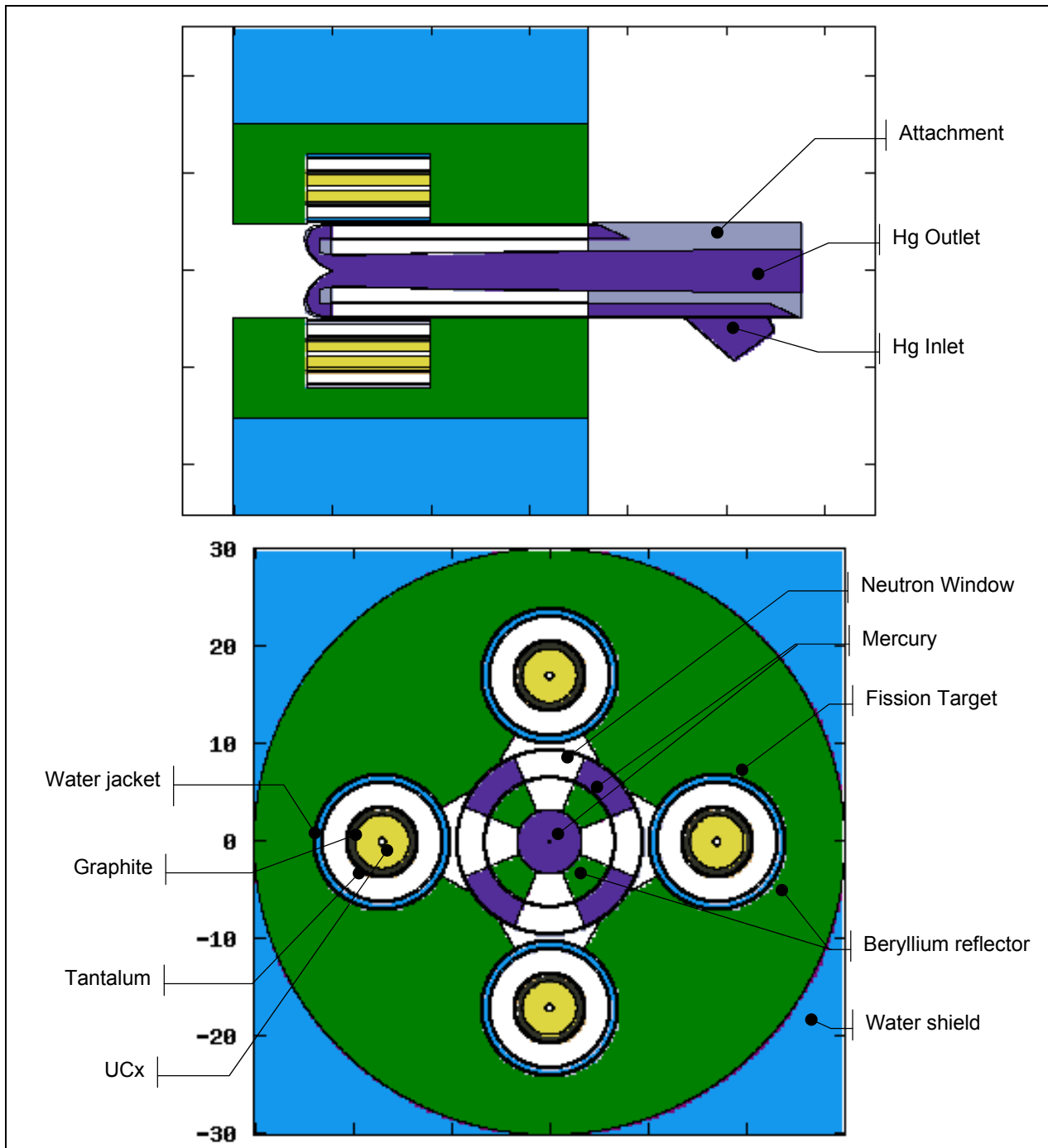

Figure 31: Optimised configuration of the Neutron source / Fission target

8.1 Isotopes produced with 4% enriched UCx

The fission yield of isotopes per MW beam power is shown on the left of Figure 32 for the entire atom range up to uranium (Z=92) and a detail for the central range of interest (Z=30 to 60). For most of the valley of stability and up to 2 atomic numbers on either side, the yield equals or exceeds the goals laid out in Table 1, and reaches 10^{13} isotopes /target /s /MW beam power. With a target volume of 500cm^3 this is equivalent to 10^{10} to 10^{11} isotopes /cm^3 /s /MW beam power
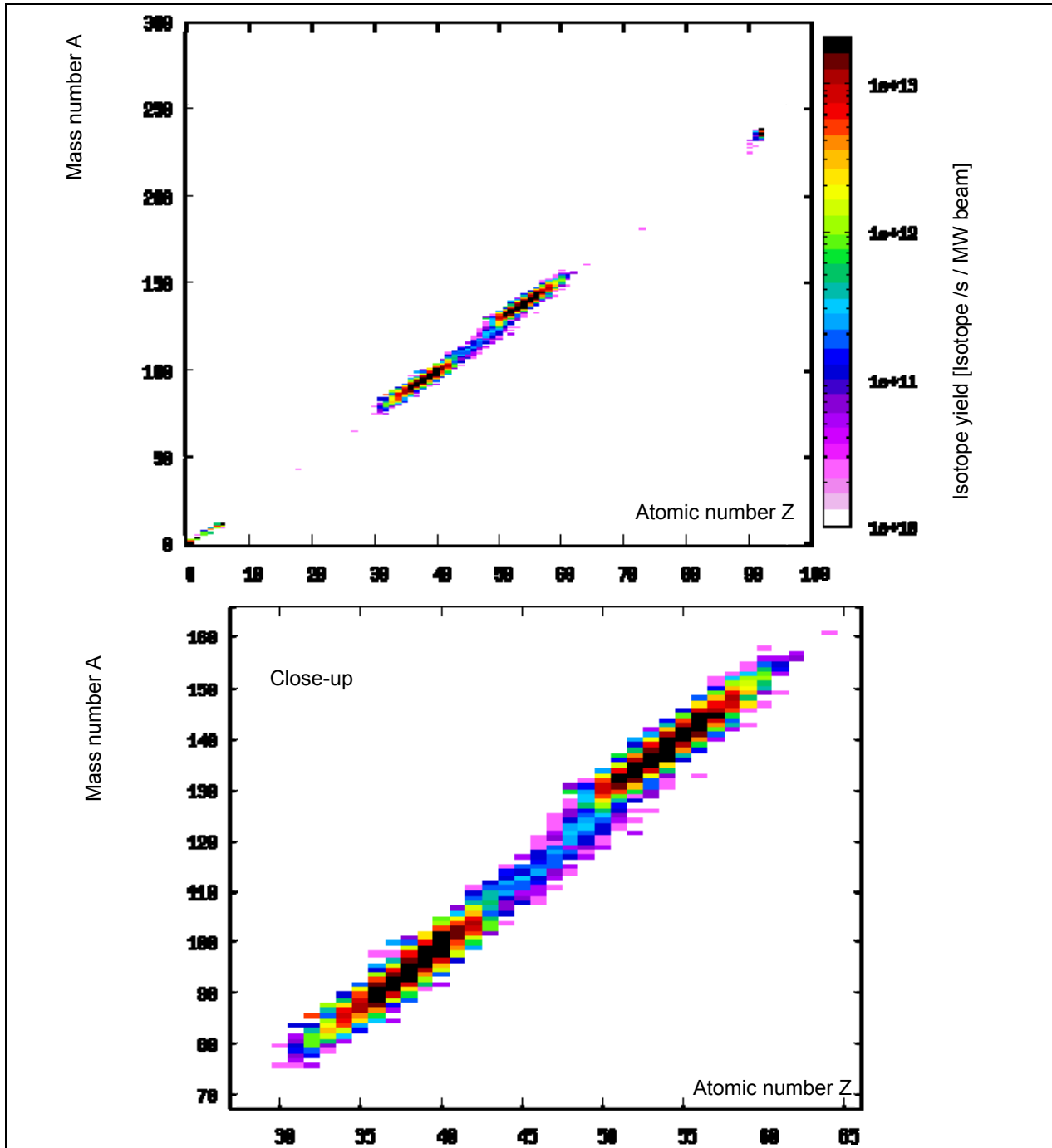

Figure 32: Isotope yield per second per target per MW beam power per target with 4% enriched uranium fission targets

The relative yield per incoming proton is depicted in Figure 33 as a function of the atomic number Z (left) and mass number A (right). These graphs are an indication of whether it is feasible to extract interesting isotopes from a given fissile material.

The possible composition of uranium available to the experimentalist ranges from depleted uranium with a U235 content lower than that of natural uranium (0.7%) to almost pure fissile U235. The latter is of course far more troublesome in terms of handling and also causes rapid burn-up which is detrimental to the safe operation of the facility. A reduction of the 4% enrichment is therefore extremely attractive, and the easiest option would be to use natural uranium. This may be a viable option and is the focus of the next section.
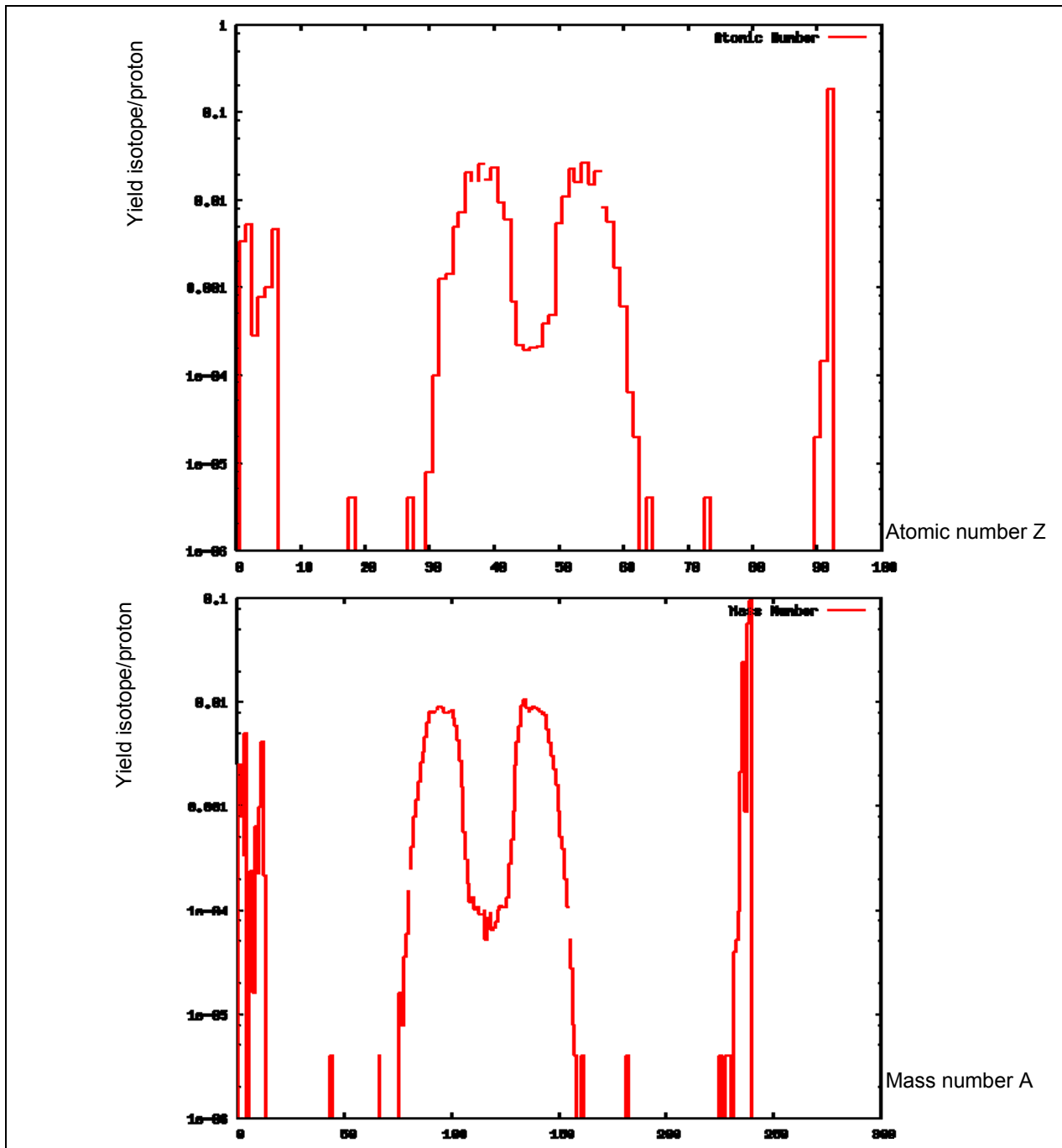

Figure 33: A and Z Isotope distribution per incoming particle with 4% enriched uranium fission targets

8.2 Isotopes produced with 0.7% natural UCx

With natural uranium, the number of fissions is reduced to 0.252 per incoming proton which amounts to 6.3×10^{15} fissions /s for a 4 MW beam. This translates into a lower yield for all isotopes, but which is not consistent with the near tenfold decrease in Uranium 235; hence the number of fissions due to the Uranium 238 is quite dominant
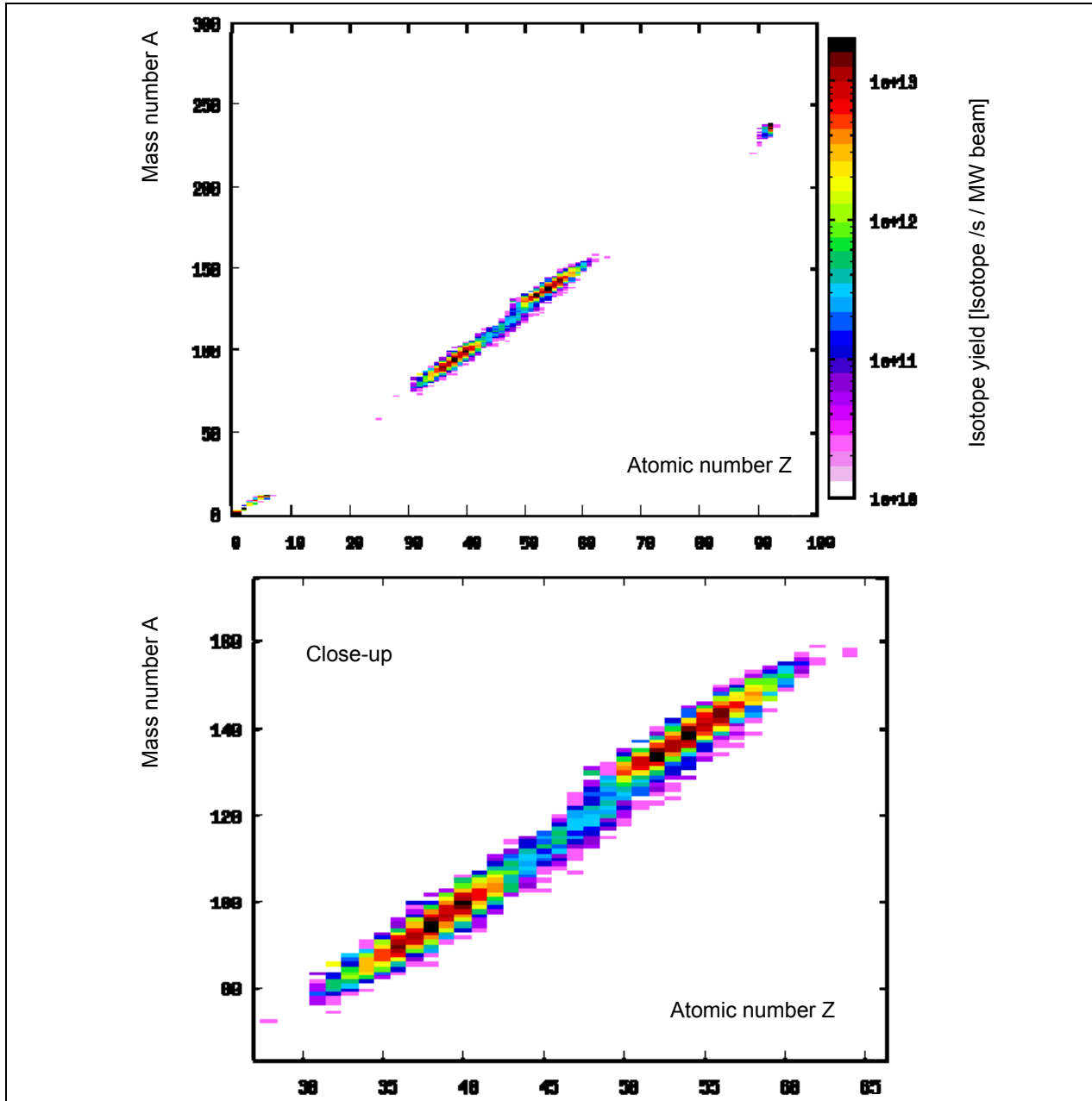

Figure 34: Isotope yield per second per target per MW beam power with natural uranium fission targets

By studying the relative strength of isotopic production in the mid range, it appears that with natural Uranium, the middle zone at Z=48 / A=125 is enhanced when compared with uranium enriched at 4%. Indeed with 4% enriched uranium, the fissile yield in this region is approximately 10^{-4} fission / incident proton, and increases to almost 10^{-3} fission / incident proton for natural uranium despite the fact that the overall fission yield is lower for

natural uranium. The additional fission in the middle range at Z=45 comes form a slight reduction in the two "humps" at Z=35 and Z = 55.

This is an indication that fast fission is indeed occurring with natural uranium, a result of the optimisation effort undertaken for integrating the new design of the converter target with dedicated fission targets.
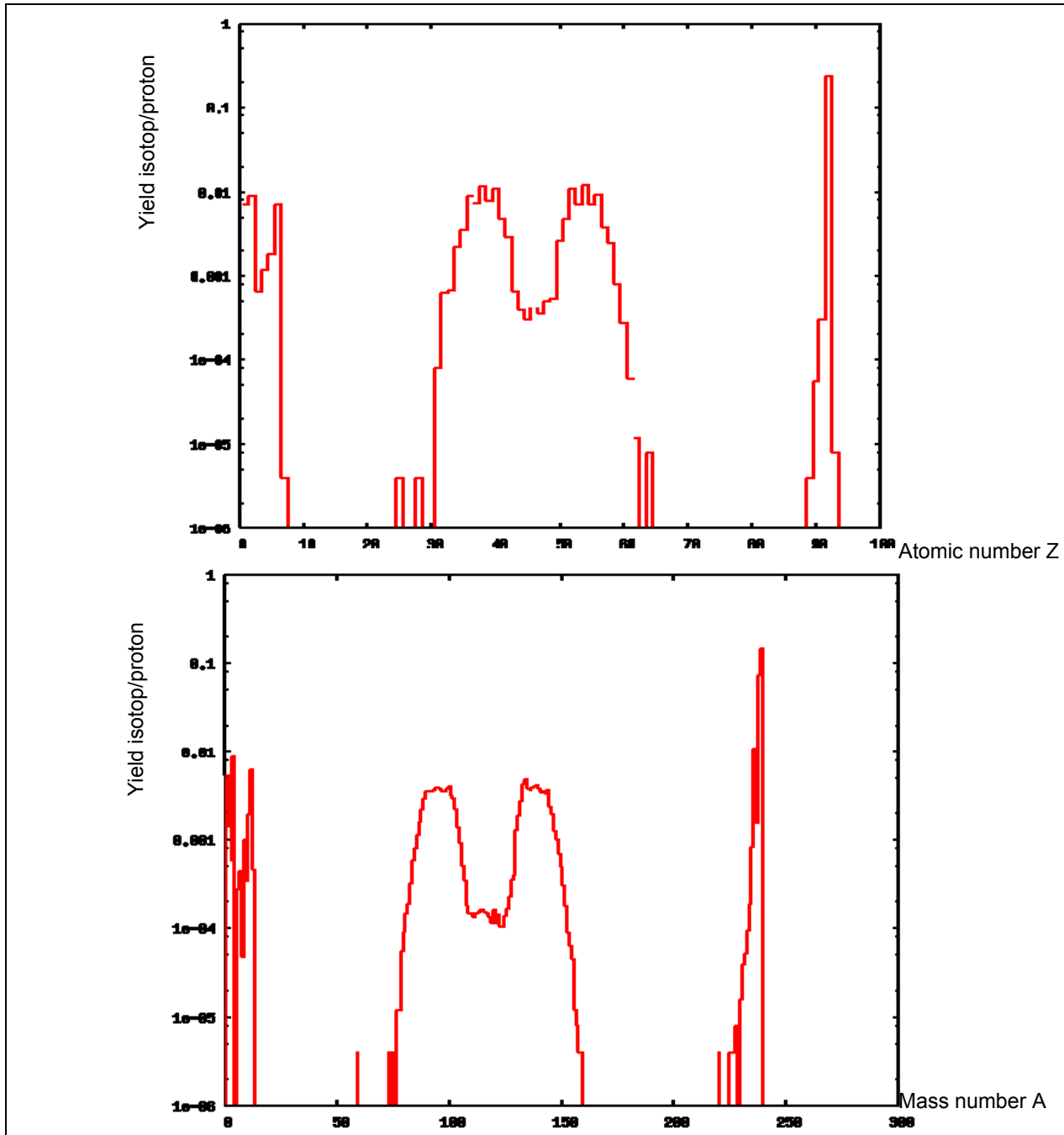

Figure 35: A and Z Isotope distribution per incoming particle with natural uranium fission targets

In terms of neutronic performance, the goal of increasing fissile yield particularly in the middle region around Z=45 has been achieved with a design which should benefit hydraulic stability.

9 Conclusion

The analysis of the base design of the neutron source initially focused on the stability of the liquid metal flow, a source of major concern due to the very high velocities reached. In order to achieve a more robust design, certain hydraulic improvements have been suggested and the impact thereof has been considered in a neutronic model with sufficient detail to examine the interaction with the surrounding structure. The neutronic model investigated the possibility of implementing a hollow guide tube as well as evacuated wedges located in the outermost annulus hence affording a passage with minimal capture to neutrons escaping the central spallation zone.

The effect of these design modifications on the neutron flux exiting the source showed a strong dependence of the local neutron flux density on the opening angle of the wedges in the income outer annulus. There is a certain degree of neutron flux concentration, which is enhanced by placing a beryllium oxide reflector material inside the hollow guide tube. Hence this configuration was retained as the baseline for further study. The number of wedges does not influence the overall production of neutrons escaping; it is only a function of the cumulated opening angle, which allows further design optimisation.

The next step involved placing fission targets at various positions and placing the wedges in a manner most likely to generate a high number of fissions. It was thus possible to demonstrate that the most favourable position for the fission targets is to place them with the longitudinal axis parallel to that of the beam axis. The region producing the greatest number of fissions was also identified by shifting the fission targets longitudinally to a position 10 cm forward of the beam window. On the other hand it seems that pointing the axis of the fission targets at right angle to the beam axis is quite detrimental to the fission yield, almost halving it.

Another advantage of the wedges was found by relocating the fission targets further afield in radial direction from the source, without causing a significant loss in fission density. This design option has possible advantages in terms of greater accessibility and better provisions for shielding, as well as lowering any criticality, a lesser concern in view of the fuel envisaged.

In terms of the variety and number of isotopes produced in the facility, it was found that the design proposed in this study would indeed allow the use of natural uranium which brings considerable improvement to the production, implementation and operation of the fission targets.